

# INTERROGATING GROUND STATE RHESUS MACAQUE AND HUMAN PLURIPOTENT STEM CELLS

by  
Sarshan Rubintheran Pather

A thesis submitted to Johns Hopkins University in conformity with the requirements  
for the degree of Master of Science

Baltimore, Maryland  
April, 2015

© 2015 Sarshan Rubintheran Pather  
All Rights Reserved

## ABSTRACT

Iterative chemical screening has resulted in optimized culture conditions to support the self-renewal of human and non-human primate pluripotent stem cells (PSCs) in a mouse embryonic stem cell-like ground state of pluripotency. While all protocols employ leukemia inhibitory factor (LIF) supplemented with MEK/ERK and GSK3- $\beta$  inhibitors (LIF 2i), many indispensably require additional anti-apoptotic small molecules and primed growth factors. The finding of a minimal cocktail of LIF 2i plus axin-stabilizing XAV939 (termed LIF 3i) that efficiently reverts select myeloid progenitor hiPSC lines to a ground state advances the possibility that among heterogeneous PSCs, many lines are epigenetically more amenable to naïve reversion than others. Here, I report characterization of LIF 3i-permissive human naïve PSCs by examining transcriptome microarray data and OCT3/4 enhancer DNA methylation profiles. Additionally, I report an optimized feeder-dependent culture system to support naïve-like self-renewal in non-permissive rhesus macaque embryonic stem cells (rESCs) derived from *in vitro* fertilization (IVF), somatic cell nuclear transfer (SCNT), and parthenogenesis. Use of a potent VEGF receptor inhibitor, sunitinib malate, together with LIF 3i or LIF 2i, promoted naïve-like ground state self-renewal in rESCs. Efficient derivation and careful interrogation of human and non-human primate naïve PSCs before *in vitro* differentiation, plasmid-based gene targeting, or blastocyst complementation experiments is a necessary process to advance naïve pluripotency in stem cell biology and regenerative medicine.



## **PREFACE**

### **Acknowledgements**

During my time in the Zambidis Lab, I have learnt how to plan and conduct experiments, and learnt how to analyze scientific data. Most importantly, I have begun my journey towards learning to think like a scientist. For this, I am forever grateful to Dr. Elias T. Zambidis (ETZ) for his superior mentorship, expertise, and support. Dr. Zambidis took me under his wing, showed faith in my abilities, and gave me a start in science. Ahead of my upcoming career in science, I could not ask for a better mentor. During our many conversions, Dr. Zambidis has taught me that to fully pursue academics as a scientist, one must understand and value knowledge boundaries formalized in the past and subsequently attempt to break those boundaries for the future. I will value these thoughts throughout my career.

I would also like to acknowledge and thank Dr. Ludovic Zimmerlin (LZ), Dr. Jeffrey Huo (JH), and Dr. Tea Soon Park (TSP) for expert technical guidance and advice. I particularly thank Dr. Jeffrey Huo for bioinformatics support. Lastly, I am grateful to Dr. Kathryn Tifft (KT) for teaching me powerful presentation and writing skills during my time in the Biology Master's Program.

This research was supported via grants provided by the Institute for Cell Engineering at the Johns Hopkins University School of Medicine (ETZ) and the Maryland Stem Cell Research Fund (ETZ).

## **Dedication**

I would like to dedicate this thesis to my parents, my sister, and my grandparents for their unwavering support and encouragement throughout my time at Johns Hopkins University. My studies would not be possible without them. I would also like to dedicate this thesis to my mentor Dr. Elias T. Zambidis.

## **Master of Science Thesis Committee**

Chair: Haiqing Zhao, PhD

Members: Robert D. Horner, PhD

Kathryn Tifft, PhD

Elias T. Zambidis, MD/PhD

## TABLE OF CONTENTS

<b>ABSTRACT.....</b>	<b>ii</b>
<b>PREFACE.....</b>	<b>iii</b>
<b>Acknowledgements .....</b>	<b>iii</b>
<b>Dedication.....</b>	<b>iv</b>
<b>LIST OF TABLES .....</b>	<b>vii</b>
<b>LIST OF FIGURES .....</b>	<b>viii</b>
<b>INTRODUCTION.....</b>	<b>1</b>
<b>On primed and naïve pluripotent stem cells in mice and non-rodents.....</b>	<b>1</b>
<b>Human stem cells with stable and authentic mouse ESC-like properties .....</b>	<b>9</b>
<b>The impact of deriving authentic ground state human and rhesus PSCs .....</b>	<b>10</b>
<i>A paradigm shifting methodology for stem cell biology and regenerative medicine .....</i>	<i>10</i>
<i>Towards improving gene targeting via plasmid-based homologous recombination .....</i>	<i>11</i>
<i>The role of XAV939 in naïve pluripotency and non-homologous end joining .....</i>	<i>13</i>
<i>Using rhesus PSCs in blastocyst complementation experiments .....</i>	<i>15</i>
<b>Hypothesis and Objectives .....</b>	<b>17</b>
<b>RESULTS .....</b>	<b>18</b>
<b>Primed rhesus embryonic stem cells (ORMES-22) display unstable morphology and pronounced tendencies to spontaneously differentiate in basic fibroblast growth factor-supplemented knockout serum media.....</b>	<b>18</b>
<b>ORMES-22 rESCs convert inefficiently to a naïve ground state of pluripotency with LIF 3i and LIF 5i cocktails .....</b>	<b>19</b>
<b>Optimization of culture conditions to support naïve-like self-renewal of rhesus embryonic stem cells with recombinant growth factors .....</b>	<b>20</b>
<b>Use of the anti-cancer drug, sunitinib malate, supports naïve-like self-renewal of converted ORMES-22 rESCs .....</b>	<b>21</b>
<b>Conversion of ORMES-22 rESCs with one passage of LIF 5i and subsequent passaging in LIF 4i supports robust naïve-like self-renewal.....</b>	<b>21</b>
<b>Direct conversion of ORMES-22 rESCs with an alternative LIF 3i cocktail supports improved self-renewal and retention of phenotypic pluripotency .....</b>	<b>23</b>
<b>Direct conversion of alternative rhesus ESC lines favors LIF 4i reversion .....</b>	<b>24</b>

<b>Authentic LIF 3i-converted human ground state PSCs display characteristic hallmarks of a stable naïve state .....</b>	<b>24</b>
<i>LIF 3i-converted ground state PSCs display activated homologous recombination machinery as determined by gene set enrichment analysis.....</i>	<i>24</i>
<i>DNA methylation does not mechanistically contribute to a potential proximal to distal enhancer regulatory switch driving OCT4 expression .....</i>	<i>25</i>
<b>DISCUSSION .....</b>	<b>27</b>
<b>Are certain PSC donors more receptive to naïve reversion than others? .....</b>	<b>27</b>
<b>Reaching a naïve ground state of pluripotency for rhesus PSCs .....</b>	<b>29</b>
<b>Examination of characteristic hallmarks for ground state pluripotency in LIF-3i converted human PSCs .....</b>	<b>32</b>
<b>CONCLUSIONS AND PERSPECTIVES .....</b>	<b>34</b>
<b>MATERIALS AND METHODS .....</b>	<b>35</b>
<b>Culture of mouse embryonic fibroblasts (MEFs) .....</b>	<b>35</b>
<b>Culture of primed rhesus monkey embryonic stem cells (rESCs) .....</b>	<b>35</b>
<b>Culture of naïve rhesus monkey embryonic stem cells (rESCs) .....</b>	<b>36</b>
<b>Monitoring phenotypic pluripotency (flow cytometry, alkaline phosphatase staining, and live fluorescent staining) .....</b>	<b>37</b>
<b>GSEA and Infinium DNA methylation array analysis.....</b>	<b>38</b>
<b>FIGURES.....</b>	<b>39</b>
<b>REFERENCES.....</b>	<b>67</b>
<b>CURRICULUM VITAE.....</b>	<b>79</b>

## LIST OF TABLES

<b>TABLE 1:</b>	A literature-based synthesis of naïve versus primed pluripotent states.....	2
<b>TABLE 2:</b>	A literature-based synthesis of current transgene-free non-rodent naïve culture conditions.....	8

## LIST OF FIGURES

<b>FIGURE 1:</b>	Species-specific contextual examination of naïve pluripotency between mice and humans.....	40
<b>FIGURE 2:</b>	The changing epigenetic and transcription factor landscape seen across the transition from naïve pluripotency to primed pluripotency.....	42
<b>FIGURE 3:</b>	Naïve pluripotency revises the clinical iPS paradigm.....	44
<b>FIGURE 4:</b>	Genome editing technologies and the ground state advantage.....	46
<b>FIGURE 5:</b>	NHEJ and the indirect depletion of DNA-PKCS by XAV939.....	49
<b>FIGURE 6:</b>	Naïve pluripotency provides a future platform for the interspecies generation of human organs in livestock animals.....	52
<b>FIGURE 7:</b>	Instability in primed bFGF/KOSR-dependent ORMES-22, CRES-2 SCNT, and rPESC lines.....	53
<b>FIGURE 8:</b>	Examination of naïve rhesus ESC domed-shaped morphology and clonal expansion post single cell passaging under different in vitro conditions.....	54
<b>FIGURE 9:</b>	Direct conversion of primed ORMES-22 p13 rESCs with one passage of LIF 5i and further passaging in LIF 3i or LIF 4i.....	56
<b>FIGURE 10:</b>	Direct conversion of ORMES-22 rESCs with varied combinations of LIF, CHIR, PD, and SU.....	59
<b>FIGURE 11:</b>	Direct conversion of alternative rhesus macaque embryonic stem cell lines derived from SCNT (CRES-2) or parthenogenesis (rPESC).....	61
<b>FIGURE 12:</b>	LIF 3i converted human pluripotent stem cells display significant enrichment in HR pathway genes.....	63

**FIGURE 13:** DNA methylation profile across the human OCT4 proximal and distal enhancer elements for high performing and low performing lines.....65

**FIGURE 14:** Possible mechanisms surrounding VEGF receptor inhibition in rhesus mESC-like self-renewal.....67

## INTRODUCTION

### **On primed and naïve pluripotent stem cells in mice and non-rodents**

A long-standing question in stem cell biology concerns the striking differences between primate and mouse pluripotent stem cells. Whether derived as embryonic stem cells (ESCs) from the inner cell mass (ICM) of blastocysts or as induced pluripotent stem cells (iPSCs) reprogrammed from differentiated somatic cells, mouse and human/non-human primate pluripotent stem cells (PSCs) exhibit pronounced phenotypic and epigenetic differences<sup>1</sup>. Cells from both species differ in their ability to integrate into the ICM of a mouse blastocyst, depend on different cytokine signaling requirements for undifferentiated self-renewal, appear morphologically distinct, and differ in their ease of single-cell cloning<sup>2</sup>. Specifically, mouse ESCs cultured *in vitro* with leukemia inhibitory factor (LIF) and small molecule inhibition of MEK/ERK and GSK3 $\beta$  (a culture cocktail termed “LIF 2i”), are preserved in a *naïve* ICM-like state<sup>3,4</sup>. Removal of LIF 2i or culture with activin/FGF promotes naïve mouse cells to drift into a *primed* pluripotent state resembling the post-implantation epiblast<sup>5</sup>. Until recently, all human pluripotent stem cell lines have existed in the primed variety. A comparison of phenotypic, molecular, and epigenetic features reveals why: naïve ICM-like mouse cells display dome-shaped morphology, utilize the distal enhancer for driving OCT4 (POU5F1) expression, exhibit global DNA demethylation, retain a pre-inactivation X chromosome state, and display H3K27me3 repressive chromatin marks on regulatory gene promoters important for development<sup>6</sup>. On the other hand, the novel discovery of primed mouse epiblast stem cells (EpiSCs)<sup>5,7</sup> has revealed that EpiSCs are remarkably similar to conventional



FGF-dependent human pluripotent stem cells. These properties include flat colony morphology, predominant utilization of the proximal enhancer to drive OCT4 expression, X chromosome inactivation, increased global DNA methylation, and acquisition of H3K27me3/bivalent domain marks on genes important for lineage commitment<sup>8,9</sup>. **Table 1** summarizes the fundamental differences between the primed (epithelial epiblast-like) and ground (ICM-like) states of pluripotency (for mice and non-rodents).

<b>Molecular, Phenotypic, or Functional Property</b>	<b>Primed (Epithelial epiblast-like)</b>	<b>Naïve (ICM-like)</b>
<b><i>In vitro</i> culture terminology</b>	Rodent EpiSCs; primate “primed” ESCs	Rodent ESCs; and primate “naïve” ESCs
<b><i>In vivo</i> embryonic tissue correlate</b>	Egg cylinder or embryonic disc	ICM or early epiblast
<b>Ability to form blastocyst chimeras</b>	No	Yes
<b>Ability to form teratomas</b>	Yes	Yes
<b>Pluripotency factors</b>	OCT4, SOX2, NANOG	OCT4, NANOG, SOX2, KLF2, KLF4
<b>Naïve Markers</b>	Absent	STELLA (DPPA3), NR5A2, REX1, NROB1, FGF4
<b>Markers of specification</b>	FGF5, T	Absent
<b>Differentiation bias</b>	Line-dependent and variable	None
<b>Effect of LIF/STAT3 signaling</b>	None	Self-renewal
<b>BMP4 responsive</b>	No	Yes
<b>Effect of FGF/ERK</b>	Self-renewal	Differentiation
<b>Effect of 2i supplementation</b>	Death and differentiation	Self-renewal
<b>Single cell clonogenicity</b>	Weak	Strong
<b>Doubling times</b>	24-26 hours	12-14 hours
<b>Morphology</b>	Flat	Dome-shaped
<b>OCT4 enhancer predominance</b>	Proximal enhancer (PE)	Distal enhancer (DE)
<b>XX status</b>	XaXa	XaXi

**Table 1: A literature-based synthesis of naïve versus primed pluripotent states**

Modified from Nichols and Smith (2009)<sup>1</sup>. Abbreviations: XaXa = both active X chromosomes; while XaXi = one active and one inactive X chromosome.

A comparison of naïve versus primed pluripotent stem cells has led many to speculate whether a naïve mouse-like state in human stem cells could be preserved *in vitro*. It is estimated that mice and humans diverged approximately 92.3 million years ago<sup>10</sup> and primarily, the challenge of deriving mouse-ESC-like cells in humans has been attributed to the peri-implantation requirement for LIF/STAT signaling during diapause, a developmental stage nonexistent in humans<sup>11</sup>. Certainly, derivation of human ground state naïve pluripotent stem cells would offer tremendous benefits for regenerative medicine. Ease of single cell cloning, rapid doubling times, likely improved *in vitro* differentiation, ability to integrate into the ICM/ability to form chimeras, and amenability for plasmid-based gene targeting via homologous recombination (HR) are some of the novel benefits promised by generating naïve human pluripotent stem cells. **Figure 1** examines the key differences between ground state pluripotency in mice and humans and depicts the various culture conditions required for deriving primed pluripotent stem cells and naïve pluripotent stem cells.

At the molecular level, what transcription factor programs mediate the phenotypic differences seen between naïve and primed pluripotent states? How can we visualize the potency of naïve pluripotency compared to primed pluripotency? **Figure 2** details the changing epigenetic landscape and transcription factor circuitry seen across the transition from naïve pluripotency to lineage segregation. Five key stages of stem cell potency are described: naïve pluripotency, a reversibility phase, a transitional state, primed pluripotency, and lineage segregation. We must appreciate that sustaining naïve human pluripotency is akin to capturing a transient stage seen during embryonic development and attempting to preserve that stage *in vitro* indefinitely. As depicted in **Figure 2A**, the natural progression for naïve cells is to lose potency over time (i.e.

lose “potential energy”). **Figure 2B** shows that the exit from the ground state is reversible until cells reach a transitional state after which naïve ES cell identity is permanently lost<sup>12</sup>. The naïve ground state represents a globally demethylated state with unique chromatin and DNA repair properties. Having globally open chromatin means that the naïve cell represents a powerful tool to extinguish differentiation bias and improve differentiation potential (notice how much “higher” along Waddington’s Epigenetic Landscape the ground state stands compared to the primed state; **Figure 2A**). When coupled together with a potentially activated HR double-strand break DNA repair system, the naïve cell represents a platform for efficient plasmid-based gene targeting via HR.

What attempts have been made recently to derive ground state stem cells? Fortunately for regenerative medicine, pragmatic genetic and chemical manipulation has allowed several groups to convert mouse EpiSCs into ground state cells<sup>13–15</sup>. In this regard, Hanna et al. have employed 2i medium (either CHIR/PD or CHIR/Kenpaullone) supplemented with exogenous transgene-based KLF4 or c-MYC<sup>13</sup>. Note that Kenpaullone (KP) is a potent inhibitor of GSK3 $\beta$  and CDK1/cyclin B<sup>16–18</sup> and the basis for choosing KP to revert mouse EpiSCs to ICM-like mESCs relies on the fact that KP is able to replace ectopic KLF4 during the reprogramming of somatic cells to iPSCs<sup>19</sup>. Similarly, Guo et al. employ KLF4 overexpression with 2i conditions<sup>14</sup>, while Silva et al. demonstrate that NANOG overexpression amidst 2i conditions is a critical determinant for conversion of EpiSCs into mESCs<sup>15</sup>. While NANOG is initially dispensable during transcription factor iPSC reprogramming to ground state iPSCs, Silva et al. demonstrate that dedifferentiated intermediates require NANOG expression to completely transition towards ground state self renewal<sup>15</sup>. Therefore,

transcriptional NANOG functions as the “gateway” to the ground state of pluripotency. Transgene-based conversion has also been achieved for human primed cells<sup>9,20</sup>. Hanna et al. demonstrate the rewiring of primed hESCs towards a naïve-like mESC state with ectopic induction of Oct4, Klf4, and Klf2 factors amidst LIF 2i medium<sup>9</sup>, and Wang et al. describe the powerful finding that overexpression of the four Yamanaka factors (OCT4, SOX2, KLF4, c-MYC) together with retinoic acid receptor gamma (RAR- $\gamma$ ) and liver receptor homolog 1 (LRH-1 or NR5A2) during the reprogramming of primary human neonatal and adult fibroblasts is able to induce mESC-like self renewal<sup>20</sup>. These ground state iPSC display growth properties, gene expression signatures, and signal dependencies that align with canonical ICM-like mESCs<sup>20</sup>.

Of interest, however, are the recent reports of transgene-free conversions of primed pluripotent human and rhesus macaque PSCs into putative naïve mouse-like cells<sup>21–27</sup>. Of these recent reports, the majority of groups employ various small molecule inhibitors and recombinant growth factors to block differentiation and stimulate LIF/STAT self-renewal (notably, JAK/STAT3 activation is sufficient to enable induction of a naïve pluripotent state even amidst antagonistic cues<sup>28</sup>). However, Ware et al. are the only group of the recent protocols to omit exogenous human LIF<sup>24</sup>. To summarize the recent transgene free naïve protocols, **Table 2** depicts individual culture conditions used by the various groups. The work of Zimmerlin et al. (2015), which is currently under review, is also included for comparison purposes. Note that of all previous transgene-free naïve conversion formulas, only the LIF 3i cocktail of Zimmerlin et al. closely parallels classical LIF 2i conditions (most groups succumb to the use of multiple complex anti-apoptotic small molecule inhibitors and primed

growth factors.) While it may seem that the cocktail of Takashima et al.<sup>26</sup> also closely parallels classical LIF 2i (they employ LIF 2i with the protein kinase C inhibitor Gö6983 that acts to suppress mouse ES cell differentiation<sup>29</sup>), the Jacob Hanna lab has found that this LIF 2i + Gö6983 combination is insufficient to produce genetically unmodified naïve human pluripotent stem cells in their hands<sup>30</sup>. One reason for this may be the genetically modified pluripotent stem cells used by Takashima et al., which use doxycycline (DOX) to drive NANOG-KLF2 expression. The NANOG and KLF2 transgenes may be leaky even in the absence of DOX and this effectively renders the transgene-free cocktail of Takashima et al. as LIF 2i/Gö6983 + leaky NANOG-KLF2 expression (which is obligatory to maintain select clones that can tolerate the somewhat harsh LIF 2i/ Gö6983 conditions).

Additionally, the cocktail of Chan et al.<sup>22</sup> also may seem to parallel classical LIF 2i conditions. While they omit primed growth factors like Zimmerlin et al., they employ the bone morphogenetic protein (BMP) signaling inhibitor Dorsomorphin. The use of Dorsomorphin here defies conventional literature describing BMP4 responsiveness in classically naïve mESCs. Ying et al. demonstrate that serum withdrawal promotes neural precursor differentiation of mESCs<sup>31</sup>; however, remarkably, exogenous BMP4 supplementation can replace serum in mESC culture (when combined with exogenous LIF) to promote ground state self renewal<sup>32</sup>. The implication here is that BMP synergistically cooperates with LIF to sustain ground state self renewal of mESCs, and while the effect of BMP alone is to promote non-neural differentiation<sup>33,34</sup>, BMP/LIF together blocks ES cell differentiation. Mechanistically, BMP suppresses the differentiation of ES cells primarily via induction of *Id* genes, which are classical basic helix-loop-helix transcription factor antagonists<sup>32,35,36</sup>. Given such information,

the use of the BMP inhibitor Dorsomorphin by Chan et al. in their human naïve formulation defies classical definitions for ground state self-renewal set forth by Austin Smith and colleagues<sup>3</sup>. It is especially intriguing that Chan et al. find that BMP inhibition supports naïve human pluripotency considering that they also employ exogenous human LIF. It is for this reason that the BMP4-responsive formulation of Zimmerlin et al. stands above the other leading protocols as the most authentic formulation to support mESC-like naïve human pluripotency (BMP4-responsiveness data is currently unpublished).

	Gafni (2013) <sup>21</sup>	Chan (2013) <sup>22</sup>	Valamehr (2014) <sup>23</sup>	Ware (2014) <sup>24</sup>	Theunissen (2014) <sup>25</sup>	Takashima (2014) <sup>26</sup>	Fang (2014) <sup>27</sup>	Zimmerlin (2015)
<b>Journal</b>	<i>Nature</i>	<i>Cell Stem Cell</i>	<i>Stem Cell Reports</i>	<i>PNAS</i>	<i>Cell Stem Cell</i>	<i>Cell</i>	<i>Cell Stem Cell</i>	<i>Under Review</i>
<b>Primary Species</b>	Human	Human	Human	Human	Human	Human	Rhesus	Human
<b>Culture Base</b>	Albumax + N2 or 20% KOSR	mTesr1 (bFGF + TGF $\beta$ )	20% KOSR	20% KOSR	N2B27	N2B27	N2 + 15% KOSR	20% KOSR
<b>MEF Feeders?</b>	Yes	Yes	No	Yes/No	Yes	Yes	Yes	Yes
<b>Naïve Growth Factors</b>	hLIF	hLIF	hLIF		hLIF	hLIF	hLIF	hLIF
<b>Primed Growth Factors</b>	TGF $\beta$							
	bFGF		bFGF	bFGF			bFGF	
					Activin A			
<b>Inhibitor Targets or Inhibitors</b>	MEKi	MEKi	MEKi	MEKi	MEKi	MEKi	MEKi	MEKi
	GSK3 $\beta$ i	GSK3 $\beta$ i	GSK3 $\beta$ i	GSK3 $\beta$ i	GSK3 $\beta$ i	GSK3 $\beta$ i	GSK3 $\beta$ i	GSK3 $\beta$ i
								XAV939
	ROCKi		ROCKi		ROCKi			
	JNKi						JNKi	
	P38i						P38i	
	PKCi					PKCi		
		BMPi						
					BRAFi			
					SRCi			

**Table 2: A literature-based synthesis of current transgene-free non-rodent naïve culture conditions**

Note that the protocol for naïve conversion using the formula of Ware et al. (2014) involves preculture with the histone deacetylase (HDAC) inhibitors butyrate and suberoylanilide hydroxamic acid. Abbreviations: KOSR = knockout serum replacement; MEF = mouse embryonic fibroblasts; hLIF = human leukemia inhibitory factor; TGF $\beta$  = transforming growth factor beta; bFGF = basic fibroblast growth factor; MEK = mitogen-activated protein kinase kinase; GSK3 $\beta$  = glycogen synthase kinase 3 beta; ROCK = rho-associated protein kinase; JNK = c-Jun N-terminal protein kinase; PKC = protein kinase C; BMP = bone morphogenetic protein; BRAF = proto-oncogene B-Raf; and SRC = proto-oncogene tyrosine-protein kinase Src.

## Human stem cells with stable and authentic mouse ESC-like properties

As depicted in **Table 2**, our group recently formulated a novel minimal naïve cocktail to convert primed human pluripotent cell lines into a mouse-like state (unpublished data, 2015). Authored by Zimmerlin, Park, and Huo et al., the work is currently under review. The cocktail consists of XAV939 (which stabilizes axin) above the classical LIF 2i formulation developed by Austin Smith and colleagues<sup>3</sup> (which consists of exogenous LIF supplemented with MEK/ERK inhibition via the action of PD0325901 and GSK3 $\beta$  inhibition via the action of CHIR99021). Of interest is the novel WNT modulation mediated by XAV939. As a chemotherapeutic agent, XAV939 globally inhibits WNT signalling<sup>37</sup> by stabilizing the  $\beta$ -catenin destruction complex; however the combination of CHIR99021 with XAV939 acts to increase cytoplasmic-nuclear shuttling of active  $\beta$ -catenin<sup>38</sup>. In similar vein, the small molecule IWR-1<sup>39</sup> (also an axin stabilizer) in combination with CHIR99021 also seems to promote human ESC self renewal<sup>38</sup>. It is interesting to note that the non-transcriptional accumulation of active  $\beta$ -catenin in the cytoplasm (together with augmented active nuclear  $\beta$ -catenin) is suggested to stabilize the naïve state via interactions with cytoplasmic NANOG and OCT4, and surface E-cadherin<sup>40,41</sup>. Zimmerlin et al. argue that a prerequisite for efficient reversion to a stable human ground state is more effective reprogramming and reduced human PSC lineage priming. They demonstrate that their optimized stromal-priming method of converting human myeloid progenitors into human iPSCs produces pluripotent donors with *de novo* activated  $\beta$ -catenin in the cytoplasm and essentially “readies” their high-fidelity pluripotent donors for efficient minimal-cocktail conversion to a ground state.



The LIF 3i cocktail of Zimmerlin et al. converts a variety of cord-blood derived human iPSC, human fibroblast iPSC, and human ESC lines into classical ground-state pluripotent stem cells with high efficiency (unpublished data, 2015). The culture conditions promote dome-shaped morphology, global DNA demethylation and reactivation of the X chromosome. Complex bioinformatics analyses of microarray data reveals that LIF 3i naïve human pluripotent cells share a global transcriptional signature that clusters with conventional ground state mouse ESCs (unpublished data, 2015). Furthermore, current attempts to differentiate stable LIF 3i ground state cells demonstrate that conversion to a naive state may result in improved multi-lineage directed differentiation potency, quality, and kinetics.

### **The impact of deriving authentic ground state human and rhesus PSCs**

As **Figure 2A** illustrates, the naïve ground state represents a favorable high point for stem cell potency *in vitro*. As regenerative medicine advances, more emphasis will be placed onto diversified cellular platforms that provide many avenues for gene correction and regenerative therapy. The generation of authentic ground state non-rodent cells speaks to this imminent need and the following three areas of gene targeting, *in vitro* differentiation, and *in vivo* organ generation are discussed below as high-impact applications of non-rodent naïve PSCs.

### *A paradigm shifting methodology for stem cell biology and regenerative medicine*

The derivation of stable ground state human stem cells pioneers new avenues for *in vitro* gene repair and directed differentiation to operate with clinically relevant efficiencies and kinetics. **Figure 3A** describes the clinical iPS cell paradigm pre-naïve

technology. Here, patient-specific iPS cells have the potential to be used for *in vitro* differentiation and drug screening/modeling; while combining gene editing of iPS cells together with directed *in vitro* differentiation creates an opportunity for patients suffering from degenerative disorders to receive gene-corrected genetically matched cell-based transplantations. Post-naïve technology, we see that this paradigm can be revised (**Figure 3B**). Given that naïve stem cells have (1) the potential to undergo more efficient gene targeting via plasmid-based homologous recombination; and (2) possess little to no differentiation lineage-bias (**Figure 2A and 2B**), incorporating a naïve reversion step into the current iPS cell paradigm may allow genome editing and directed differentiation to operate with clinically relevant quality, potency, and kinetics. Presumably, the globally open chromatin landscape of naïve cells allows homologous recombination machinery favorable access to DNA (to allow potentially more efficient gene targeting over their primed counterparts) and similarly, the global “high point” of the naïve stem cell may extinguish any line-dependent lineage-bias during directed differentiation.

#### *Towards improving gene targeting via plasmid-based homologous recombination*

While yet to be definitively shown, reversion to an authentic naïve state likely confers increased amenability for gene editing via plasmid-based homologous recombination (HR). Since the revolution of gene targeting in mouse ESCs pioneered by Mario R. Capecchi, Martin J. Evans, and Oliver Smithies, the belief was that gene targeting using electroporated linearized plasmid constructs (**Figure 4A**) would transition seamlessly into human pluripotent cells for mechanistic studies, disease-specific modeling, and transplantation therapy. However, conventional primed plasmid-based gene targeting frequencies in human pluripotent cells have been low<sup>42–46</sup>. The belief

for the low efficiency of HR is two-fold: (1) primed cells have a tighter global chromatin structure (due to increased DNA methylation) and therefore HR machinery cannot access requisite DNA sequences with ease and (2) primed cells exhibit reduced capacity for gene targeting due to a more active non-homologous end joining (NHEJ) pathway<sup>47</sup> (the competing pathway in double-strand break DNA repair). While helper-dependent adenoviral vectors (HDAVs) with large 36 kb cloning capacities<sup>48</sup> have the ability to deliver large targeting constructs into pluripotent stem cells and overcome limitations of weak HR in primed cells, the construction of HDAVs is labor-intensive and technically challenging, and often HDAVs may permanently integrate into the genome to pose an oncogenic threat<sup>49</sup> (**Figure 4A**). In order to solve the weak HR capability of primed PSCs, researchers have turned to using synthetic nucleases to create sequence-specific double-strand breaks in human primed PSCs. In the presence of a single-stranded or double-stranded donor sequence, primed cells will more efficiently carry out HR at a synthetic break site (compared to no DSB). Zinc-finger nucleases (ZFNs), transcription activator-like effector nucleases (TALENs), and the leading RNA-guided candidate, clustered regularly interspaced short palindromic repeat-associated nuclease 9 (CRISPR-Cas9) technology are three nuclease-assisted methods currently employed in genome editing applications (**Figure 4A**). ZFNs and TALENs, which are prone to induce off target effects, are modular proteins with DNA binding domains and *FokI* nuclease activities<sup>49</sup>, while the more specific RNA-guided Cas9 nuclease offers greater genome editing precision and efficiency.

When plasmid-based homologous recombination is employed in primed cells, electroporated constructs follow one of two fates: either targeted integration via HR,

or random integration via NHEJ (**Figure 4B**). Synthetic nuclease-induced repair either follows homology-directed repair (HR), to create sequence-specific edits, or error prone NHEJ, which often induces mutational insertions and deletions or indels (**Figure 4C**). Given the complexity associated with working with ZFNs, TALENs, or CRISPR-Cas9 technologies, and the fact that these technologies are prone to off target effects, classical plasmid-based HR still represents an effective way to precisely edit the genome. Here, the naïve pluripotent advantage paves the way for re-introduction of plasmid-based HR into human PSC genome editing. While primed PSCs possess tighter chromatin and endogenous enzymatic machinery biased towards NHEJ (**Figure 4D**), naïve PSCs likely possess looser chromatin and endogenous DSB DNA repair machinery biased towards HR (**Figure 4E**). It is for this reason that naïve PSCs represent a promising target for gene correction.

#### *The role of XAV939 in naïve pluripotency and non-homologous end joining*

Does the naïve background offer further benefits for gene targeting via homologous recombination? Examination of the LIF 3i culture conditions for naïve reversion from Zimmerlin et al. reveals that the singular use of XAV939 may offer potential benefits for HR in the naïve background. While primarily used to mediate axin-stabilization and subsequent accumulation of non-transcriptional activated  $\beta$ -catenin in the cytoplasm (which is important for reversion to a stable mouse ESC-like naïve state), XAV939 inhibits poly-ADP-ribosylating enzymes tankyrase 1 (TNKS1) and tankyrase 2 (TNKS2)<sup>37</sup>. As *bona fide* poly(ADP-ribose) polymerases (PARPs)<sup>50,51</sup>, TNKS1 and TNKS2 have diverse cellular roles. Of interest to gene targeting, however, is the relationship between TNKS1 and DNA-dependent protein kinase (DNA-PK) catalytic subunit (DNA-PKCS). Under normoxic conditions, **Figure 5A**

illustrates that in connection with NHEJ, DNA-PKCS is recruited to a DNA DSB site. At the same DSB site, HR competes with NHEJ to repair the break (HR is preferentially active during S and G2 phases of the cell cycle, while error prone NHEJ can be used within any phase of the cell cycle). Within 1-6 hours after recognition of DNA damage, HR and NHEJ proteins are recruited to repair the DSB<sup>52</sup>. Within the NHEJ pathway alone, DNA-PKCS plays a critical role in the initial phases of repairing a DSB and acts to recruit key ligases and processing enzymes to the damage site<sup>53</sup> (**Figure 5B**).

Given that HR and NHEJ are in competition to repair a DSB (particularly in S and G2 phases of the cell cycle), it is apparent that suppression of NHEJ would preferentially favor HR-based repair and lead to improved targeted integration frequencies for gene targeting vectors. Here, use of XAV939 in the naïve cocktail of Zimmerlin et al. may play a powerful role. As a potent inhibitor of TNKS1, XAV939 acts to indirectly inhibit NHEJ<sup>54</sup> via depletion of DNA-PKCS, and therefore, may improve gene targeting efficiencies in human PSCs converted with LIF 3i (compared to other naive conversion cocktails which do not employ XAV939). Interestingly, XAV939-mediated DNA-PKCS depletion is equivalent to TNKS1 knockdown (in terms of depletion levels and depletion rate)<sup>37</sup>. **Figure 5C** illustrates the complete mechanism of XAV939-mediated inhibition of NHEJ. While enhanced gene targeting in the LIF 3i XAV939-supplemented background (compared to the bFGF primed background) needs validation, it is interesting to note that the naturally occurring plant-derived compound vanillin (4-hydroxy-3-methoxybenzaldehyde), when administered in combination with recombinant adeno-associated viral (rAAV) vectors, acts to increase gene targeting frequencies by 10-fold compared to control rAAV

administrations<sup>55</sup>. Derived from the pods of *Vanilla planifolia*, *Vanilla tahitensis* and *Vanilla pompon*, vanillin also acts to inhibit NHEJ by directly inhibiting DNA-PKCS<sup>56</sup>. The fact that vanillin sensitizes cells to the toxic effects of DNA-damaging agents<sup>57</sup> and is an effective antimutagenic agent<sup>58–61</sup> speaks to the notion that NHEJ is globally inhibited upon DNA-PKCS inhibition. XAV939 has the potential to have the same effect as vanillin to improve plasmid-based integration frequencies in LIF 3i converted hPSCs (**Figure 5C**).

#### *Using rhesus PSCs in blastocyst complementation experiments*

In the near future, the use of non-human primate naïve PSCs in blastocyst complementation experiments<sup>62</sup> will take us one step closer to generating human organs in organogenesis-disabled livestock (**Figure 6A**). By injecting patient-specific iPSCs into knockout-blastocysts from livestock (i.e. *Pdx1*-disabled blastocysts; *Pdx1* functions as a master regulator of pancreatic development), patient-specific iPSCs may complement the deficiency in an interspecies chimera and the newly formed organ (i.e. the pancreas in this example), would be composed entirely of genetically-matched patient cells ready for harvest and patient transplantation. While blood vessels, nerves, and interstitial cells may be chimerized between host and donor cells, perhaps by further engineering double or triple knockout blastocysts to prevent the formation of host vasculature or nerves, these issues could possibly be solved. As an alternative to blastocyst complementation, Nakauchi and colleagues propose of *in utero* conceptus complementation, where temporospatial-specific injection of committed progenitor cells generated by *in vitro* directed differentiation could allow complementation of organ deficiency without risk of any off-target effects<sup>62</sup> (**Figure 6B**). In particular, naïve pluripotency provides a further advantage by possibly

mediating the generation of high quality committed progenitors after *in vitro* differentiation (compared to lineage-skewed primed PSCs).

While these experiments may seem far off, naïve pluripotency has brought us closer to realizing the generation of interspecies chimeras. Current non-rodent PSCs of the epiblast-like primed variety are unable to contribute to chimeric animals. Mitalipov and colleagues have shown that injection of primed rhesus ESCs into blastocysts fails to produce chimeric offspring (they did, however, show that whole four-cell embryo aggregation of totipotent cells can result in the generation of chimeric monkeys)<sup>63</sup>. Using transgene-free naïve iPSCs arrested at an ICM-like stage of development with specific signaling inhibitors and stimulation of LIF/STAT signaling solves the issue of primed cells failing to contribute to chimeric offspring.

If previous experiments are any indications of success (rat-mouse chimera-generated pancreas<sup>64</sup>, mouse-mouse chimera-generated kidney<sup>65</sup>, rat-mouse chimera-generated thymus<sup>66</sup>, pig-pig chimera-generated pancreas<sup>67</sup>, and mouse-mouse chimera-generated pancreas<sup>68</sup>), a functional whole organ composed of rhesus macaque tissue grown in a livestock animal will be demonstrated soon. While issues of organ vasculature, immune rejection, and various ethical challenges must be addressed, the potential of naïve PSCs in whole organ generation holds unique and exciting promises for regenerative medicine.

## Hypothesis and Objectives

Given the widespread regenerative potential for authentic ground state rhesus PSCs, our group has recently turned to converting rhesus ESCs into a stable naïve state. Unpublished experiments indicate that LIF 3i reversion is insufficient to convert rhesus macaque ESC to a stable ground state, and therefore, further experimentation is required to optimize culture conditions. Here I investigate new *in vitro* culture conditions to support ground state growth of three rhesus macaque cell lines: ORMES-22 rhesus ESCs<sup>69</sup>, CRES-2 rhesus ESCs derived from somatic cell nuclear transfer (SCNT)<sup>70</sup> and rhesus ESCs derived via parthenogenesis (rPESCs)<sup>71</sup>. Given recent evidence that singular blocking of vascular endothelial growth factor (VEGF) signaling with sunitinib malate (SU) promotes undifferentiated mouse ESC self-renewal in the absence of feeder cells or LIF<sup>72</sup>, I hypothesize that blocking VEGF signaling in rhesus ESCs may reinforce mouse-like self-renewal. Additionally, to further confirm validity of a stable human ground state, I report microarray analysis of DNA double-strand break repair pathways in naïve human cells, together with analysis of OCT4 proximal and distal enhancer DNA methylation profiles.



## RESULTS

### **Primed rhesus embryonic stem cells (ORMES-22) display unstable morphology and pronounced tendencies to spontaneously differentiate in basic fibroblast growth factor-supplemented knockout serum media**

ORMES-22 rESCs derived from *in vitro* fertilization were cultured on mitotically inactivated mouse embryonic fibroblasts (MEFs) in knockout serum replacement (KOSR) supplemented media with 20 ng/mL basic fibroblast growth factor (bFGF). These cells exhibited typical “primed” pluripotent characteristics. Colonies were flat and exhibited pronounced tendencies to spontaneously differentiate towards fibroblastic lineages (**Figure 7**). Compared to CRES-2 SCNT and rPESC lines cultured under identical primed bFGF-conditions with KOSR, the ORMES-22 line displayed most instability (**Figure 7**). Over the course of spontaneous differentiation, the rESCs exhibited reduced expression of surface pluripotency markers TRA-1-81, TRA-1-60, and SSEA-4, as measured by flow cytometry (personal correspondence, LZ). The cells were cultured under low O<sub>2</sub> hypoxic conditions and manually passaged in colony clumps with the addition of 10  $\mu$ M rho-associated protein kinase (ROCK) inhibitor (Stemolecule Y27632). Partial-single cell dissociation during passaging resulted in pronounced differentiation and cell death even with the addition of ROCK inhibitor (data not shown). Given the unstable nature of the ORMES-22 rESCs, conversion to a naïve ground state would dramatically enhance ease of *in vitro* culture for downstream gene targeting and differentiation.

## **ORMES-22 rESCs convert inefficiently to a naïve ground state of pluripotency with LIF 3i and LIF 5i cocktails**

Given that the large majority of permissive human PSC donors (high fidelity stromal primed cord blood iPSC and H9 ESC lines) could convert efficiently with LIF 3i or LIF 5i cocktails (see below for cocktail compositions), we tested the potential of these small molecule combinations to convert ORMES-22 rESCs to an authentic naïve ground state. In order to test whether our minimal inhibitor cocktail of human LIF, supplemented with GSK-3  $\beta$  inhibitor (CHIR99021), MEK/ERK inhibitor (PD03259010) and WNT modulator XAV939 (collectively termed LIF 3i) would support the growth and derivation of naïve-like rESCs, high quality primed cells cultured to confluency over many passages were single cell dissociated with Accutase and cultured in LIF 3i. Over the course of 12 passages, the cells showed poor morphology and slow proliferation (**Figure 8A-left**). To examine whether a single passage of LIF 3i supplemented with two additional inhibitors (forskolin and purmorphamine - collectively now termed LIF 5i) would improve self-renewal, primed rESCs were converted with one passage of LIF 5i and then cultured thereafter continuously in LIF 3i. Cells showed improved morphology and growth but still displayed weak single cell cloning (**Figure 8A-right**). While morphology was good, the cells displayed reduced TRA-1-81, TRA-1-60, and SSEA-4 (personal correspondence, LZ) but still expressed the naïve markers Stella/DPPA3 and NR5A2 (personal correspondence, LZ). This indicates that even when supplemented with the protein kinase A pathway agonist forskolin (which acts to induce KLF4 and KLF2 expression<sup>9</sup>), and the hedgehog activator purmorphamine, molecules collectively expected to block differentiation and support self-renewal, the converted rESCs could not classically self-renew. Furthermore, direct conversion of ORMES-22 rESCs with

LIF 5i resulted in noted monolayer fibroblastic-like differentiation after 4-5 passages post single cell dissociation and culture in LIF 5i (personal correspondence, LZ).

### **Optimization of culture conditions to support naïve-like self-renewal of rhesus embryonic stem cells with recombinant growth factors**

Given that direct LIF 3i, combined LIF 5i to LIF 3i, or direct LIF 5i conversion attempts with ORMES-22 rESCs were primarily unsuccessful owing to weak self-renewal and unstable retention of phenotypic pluripotency over long-term culture (greater than 5 passages post conversion), I attempted to optimize growth of converted rESCs with recombinant growth factors above basal LIF 3i media. LIF 3i culture media was supplemented with further recombinant growth factors to examine whether the converted rESCs could be resurrected from a state of weak self-renewal. Given evidence that hypoxia promotes PSC renewal<sup>73</sup>, and the fact that primed ORMES-22 cells are conventionally cultured under low oxygen tensions, the addition of bFGF and BMP4 was examined under both normoxic and hypoxic conditions. The addition of bFGF greatly improved cell growth more than 3-fold under normoxic conditions and near 5-fold under hypoxic conditions (**Figure 8B**). The microenvironment ‘niche’ effect produced by hypoxia and the addition of bFGF is not surprising: conventional primed rESCs proliferate freely under low oxygen tensions. The fact that after LIF 5i to LIF 3i conversion and continued passaging in LIF 3i the cells do not respond to either hypoxia (without additional growth factors) or BMP4 (**Figure 8B**) indicates that the addition of bFGF probably converts the cells into a quasi-naïve or “super” primed state, from which they respond significantly to hypoxia (as do ORMES-22 primed rESCs). Notably, LIF 3i-converted human pluripotent stem cells are BMP4-responsive and classically naïve (unpublished data, 2015).

### **Use of the anti-cancer drug, sunitinib malate, supports naïve-like self-renewal of converted ORMES-22 rESCs**

In an effort to definitively resurrect the converted rESCs without primed growth factors (i.e. bFGF, SCF, TGF- $\beta$ ), I reasoned that combined inhibition of various receptor tyrosine kinases (RTKs) including VEGF receptor and PDGF receptor would promote naïve-like self-renewal (given that singular blocking of VEGF signaling promotes undifferentiated mouse ESC self-renewal in the absence of feeder cells or LIF<sup>72</sup>). The chosen molecule sunitinib malate (SU11248 or SU), a potent inhibitor of VEGF receptor, PDGF receptor, KIT, FLT3 and RET, was tested on top of LIF 3i under normoxic and hypoxic conditions. LIF 3i plus 1  $\mu$ M sunitinib (termed LIF 4i) produced improved single cell growth under hypoxic conditions (**Figure 8C**), which is interesting considering that hypoxia inducible factor-1 alpha (HIF-1  $\alpha$ ) lies downstream of VEGF receptor. Removal of LIF in LIF 4i conditions (termed 4i alone), showed improved but weak growth under hypoxia versus the control LIF 3i (**Figure 8C**).

### **Conversion of ORMES-22 rESCs with one passage of LIF 5i and subsequent passaging in LIF 4i supports robust naïve-like self-renewal**

In order to assess the efficacy of SU and the GSK3 $\beta$  inhibitor lithium chloride<sup>74</sup>, fresh primed bFGF-dependent rESCs were converted with one passage of LIF 5i and then cultured in either LIF 3i, LIF 4i, LIF 3i plus lithium chloride, or LIF 4i plus lithium chloride (all under hypoxic conditions). **Figure 9A** details a general conversion protocol. After one passage in LIF 5i, the ORMES-22 rESCs displayed naïve-like dome-shaped morphology and proficient growth (**Figure 9B**). However, the cells displayed weak TRA-1-81 expression as determined by flow cytometry, and low

SSEA-4 expression on the order of 10% SSEA-4<sup>+</sup> cells (**Figure 9Fi, G**). A switch to either LIF 3i or LIF 4i did not improve SSEA-4 surface marker expression, which fell to almost zero after 2 passages in either LIF 3i or LIF 4i (**Figure 9Fii, Fiii, G**). Despite this, cell growth was markedly improved in LIF 4i conditions compared to the other tested culture conditions (**Figure 9C**). It appears that the addition of 1  $\mu$ M sunitinib was keeping the converted cells in a proliferative state, even after the stress of single cell dissociation. Growth in LIF 4i appeared to have an improved effect after the second passage, with an improved rate of growth (**Figure 9D**).

While the converted cells cultured in LIF 3i or LIF 4i displayed reduced expression of pluripotency surface markers, it is possible that the human conjugated antibodies used for flow cytometry were not reacting to the markers on rhesus cells. Additionally, it is possible that the starting population of bFGF-dependent cells were already in the process of differentiation prior to conversion. Therefore, to assay pluripotency further, converted cells cultured in LIF 3i or LIF 4i were examined for expression of alkaline phosphatase. All pluripotent stem cells exhibit elevated expression of alkaline phosphatase. While some ORMES-22 LIF 5i to LIF 3i rESCs stained positive for alkaline phosphatase (**Figure 9E-centre**), most of these colonies displayed differentiated morphologies and so were regarded as false positives (**Figure 9E-centre**). ORMES-22 LIF 5i to LIF 4i rESCs displayed robust staining for alkaline phosphatase and even small colonies stained positive (**Figure 9E-right**), highlighting that rESCs cultured in LIF 4i were highly clonogenic and undifferentiated.

### **Direct conversion of ORMES-22 rESCs with an alternative LIF 3i cocktail supports improved self-renewal and retention of phenotypic pluripotency**

For naïve pluripotency to have an immediate impact on regenerative medicine clinically, naïve conversion protocols must be simple, uncontrived, and efficient. As such, direct conversion of PSCs with unique minimal inhibitor cocktails is desirable to ensure widespread protocol adoption in translational research or therapy. In order to examine whether LIF 5i-initial conversion was dispensable, I converted ORMES-22 cells directly using 12 different conditions (6 conditions under normoxia and 6 conditions under hypoxia; **Figure 10A**). Most notably, an alternative LIF 3i (with CHIR, PD, and SU) under normoxic conditions supported the highest growth rates (**Figure 10A**). Cells under similar conditions under hypoxia showed slower growth rates but better morphology after one passage (**Figure 10B**). However, given the rapid growth rates under normoxic LIF CHIR-PD-SU conditions, it is possible that this condition promotes discreet differentiation of the ORMES-22 cells. Indeed, at passage 2, this alternative LIF 3i combination appears to have promoted differentiation under both normoxia and hypoxia (**Figure 10C**), as evidenced by monolayer-like morphology and little to no SSEA-4 surface marker expression (**Figure 10D**). Interestingly, classical LIF 2i showed good growth kinetics over two passages (**Figure 10A, E**) and surprisingly good morphology (**Figure 10B, C**). However, this condition also resulted in poor SSEA-4 expression (**Figure 10D**). At this stage of the experiment, the novel secondary LIF 3i (LIF XAV-PD-SU) under normoxia appears to have moderate growth rates, but importantly seems to cause strong retention of SSEA-4 expression (**Figure 10D**). Note that hypoxia appears to buffer the growth kinetics seen across the six culture conditions versus normoxia (tighter distribution of curves in **Figure 10E-right** compared to normoxia in **Figure 10E-left**).

### **Direct conversion of alternative rhesus ESC lines favors LIF 4i reversion**

CRES-2 SCNT rESCs together with parthenogenesis-derived rPESCs were also converted directly without LIF 5i to determine if particular rESC lines are more permissive to naïve reversion than others. CRES-2 cells showed poor growth and weak SSEA-4 expression under hypoxic LIF 3i or LIF 4i conditions (**Figure 11A, B, C, D**), while rPESCs showed stronger growth and moderate SSEA-4 expression under LIF 4i compared to LIF 3i (**Figure 11A, B, C, D**). This is confirmed by the longitudinal examination of growth kinetics. At this stage, only the rPESC LIF 4i line appears to be expanding successfully (**Figure 11E**) compared to the three other experimental samples.

### **Authentic LIF 3i-converted human ground state PSCs display characteristic hallmarks of a stable naïve state**

*LIF 3i-converted ground state PSCs display activated homologous recombination machinery as determined by gene set enrichment analysis*

In order to examine whether conversion to a naïve state of pluripotency may support more efficient gene targeting via homologous recombination (HR), gene set enrichment analysis (GSEA)<sup>75</sup> of gene expression array data was employed. Illumina HumanHT-12 arrays previously conducted on 12 different naïve ESC and iPSC lines, together with their primed source cells (from Zimmerlin et al.), were analyzed to examine differences in HR genes and NHEJ genes. GSEA is a bioinformatics computation that examines whether an *a priori* defined set of genes shows statistically significant differences between two different biological states (here naïve vs. primed). HR pathway genes were upregulated in the naïve state with a normalized enrichment score (NES) of 1.42 with a significant p value < 0.05 for all lines (**Figure 12A**).

Notably, stromal primed cord blood iPSC lines appear to show the most robust upregulation of HR pathway genes in the naïve state. NHEJ pathway genes were also upregulated with an NES of 0.95 in the naïve state, however this result was not statistically significant (**Figure 12B**). This indicates that the naïve ground state in human pluripotent stem cells is potentially amenable to support more efficient plasmid-based gene targeting via endogenously-activated HR machinery.

*DNA methylation does not mechanistically contribute to a potential proximal to distal enhancer regulatory switch driving OCT4 expression*

Given that the distal enhancer of OCT4 predominantly drives OCT4 expression in the naïve state, I sought to investigate whether LIF 3i converted human cells displayed DNA methylation changes across the distal or proximal enhancers in comparison to bFGF source cells. While it is likely that a combination of histone modifications and DNA methylation changes drive the switch from proximal to distal enhancer regulation during the primed to naïve transition, DNA methylation may play a dominant mechanistic role in this transition. Previously conducted Infinium 450k methylation arrays from the work of Zimmerlin et al. (2015) were probed to examine any DNA methylation differences across the OCT4 proximal or distal enhancer between naïve and primed human PSC lines. As defined by Zimmerlin et al. (2015), “high performing lines” were human ESC and stromal-primed myeloid progenitor iPSC primed lines that converted efficiently with LIF 3i as measured by naïve growth characteristics, retention of phenotypic pluripotency, and naïve hallmarks. “Low performing lines” were fibroblast iPSC primed lines that converted inefficiently with LIF 3i as measured by the above criteria. The Infinium 450k array provides six CpG probes in the proximal enhancer, and three probes in the distal enhancer (**Figure 13**).



Note that the proximal and distal enhancer coordinates along human chromosome 6 were extracted using sequence homology to two luciferase proximal enhancer and distal enhancer constructs (see Gafni et al.<sup>21</sup>). These constructs will be used in a future functional OCT4 enhancer predominance assay and it was important for us to examine methylation profiles at endogenous sequences that paralleled sequences found in OCT4 luciferase enhancer vectors. This way, any differences in downstream results (from DNA methylation profiling versus functional profiling with luciferase constructs) can be appropriately compared given that the endogenous enhancer sequences and construct enhancer sequences perfectly align. Unexpectedly, for both high performing lines and low performing lines, the bFGF primed source cells on average displayed greater methylation at the proximal enhancer compared to LIF 3i cells (**Figure 13**). However, it is interesting to note that at CpG sites 5 and 6, low performing LIF 3i lines display higher methylation levels at the proximal enhancer (which is somewhat indicative of a putative naïve state). At the distal enhancer, the methylation profile is more indicative of the naïve state. Both high performing and low performing LIF 3i lines display reduced methylation versus their bFGF source counterparts, indicating some level of distal enhancer activity. While experiments such as ChIP-PCR or DNase I hypersensitivity assays will allow further examination into OCT4 enhancer regulation, functional assessment of enhancer predominance (i.e. through luciferase reporter constructs) is needed to fully conclude whether or not LIF 3i human conversion results in the typical proximal to distal enhancer switch.

## DISCUSSION

### **Are certain PSC donors more receptive to naïve reversion than others?**

Considering the fact that select human stromal primed cord blood iPSC lines revert more efficiently to a naïve state with LIF 3i compared to fibroblast iPSC (unpublished data, 2015), we can establish that receptiveness to naïve reversion is line-dependent. This may stretch across species. Indeed, *in vitro* phenotypic and molecular heterogeneity coupled with interline variability dominates the culture of mouse, human, and rhesus macaque pluripotent stem cell (PSC) culture. As measured by defined performance metrics for pluripotency (including differentiation potency and phenotypic and functional pluripotency), studies have identified (notably in human cells) that it is unclear whether unique genetic or epigenetic differences between ESC lines<sup>76–79</sup> and iPSC lines<sup>80–84</sup> contributes to variability. Presumably, distinct derivation methods, culture reagents, passaging techniques, choice of mitotically inactivated feeder cells, and atmospheric conditions used to expand PSCs causes unique cell lines to fall within distinct brackets on the classically defined epigenetic continuum of differentiation first described by Conrad Waddington in 1957<sup>85,86</sup>. Simply, receptiveness to naïve reversion may depend on a starting cell's “epigenetic distance” from the canonical ground state.

At the top of Waddington's landscape we find the ground state of PSC self-renewal (LIF/JAK/STAT3, BMP4 responsive<sup>3,32,87,88</sup>), and following a further committed trajectory downhill, the primed PSC state of self-renewal (bFGF, Activin A responsive). Given the complex cocktails of primed growth factors and viability enhancers used to sustain supposedly naïve mouse-ESC-like human pluripotency, and

the recent report of rhesus macaque naïve iPSCs converted with LIF 2i/bFGF<sup>27</sup>, it is possible that human and non-human primate primed PSCs are “non-permissive” to conversion to a canonical ground-state defined by mouse-ESCs. However, our lab has recently shown that stromal-primed STAT3-activated human CD33<sup>+</sup>CD45<sup>+</sup> myeloid progenitors reprogrammed to a state of induced pluripotency with little to no reprogramming aberrations are amenable to ground-state reversion with LIF 2i supplemented with XAV939. Given this and further evidence that PSCs reprogrammed from somatic cells may assume distinct pluripotent states within the upper echelons of Waddington’s epigenetic landscape<sup>89</sup>, it is clear that species-specific differences are not the only reasons for the previously difficult conversion of human and non-human primate PSCs into a BMP4 responsive ground state.

Data presented indicates that the ORMES-22 rESC line used in this study is non-permissive to minimal-cocktail naïve reversion. The line was derived in fetal bovine serum (FBS) culture media<sup>69</sup> and definitively requires high concentrations of bFGF to eliminate spontaneous differentiation. Upon receipt of the line from Shoukhrat Mitalipov, our lab adapted the line to knockout serum replacement (KOSR). It is possible then, that the primed ORMES-22 line requires growth factors present in FBS (which are absent in knockout serum) to proliferate in a continued undifferentiated state. ORMES-22 primed rESCs will likely need to be cultured in FBS-supplemented media over multiple passages (>10) to realize whether the cells are experiencing an FBS-deficiency after KOSR adaptation.

## Reaching a naïve ground state of pluripotency for rhesus PSCs

Previous conversion attempts in our lab with LIF 3i or LIF 5i have shown that the ORMES-22 line shows growth kinetics that aligns with previously defined non-permissive hESC lines (including H7 and ES03). Interestingly, unpublished bioinformatics analyses of global transcriptional profiles do not reveal any striking reason for why the H7 and ES03 hESC lines convert inefficiently with LIF 3i or LIF 5i (personal correspondence, LZ and JH). Given that LIF 3i/LIF 5i-converted ORMES-22 rESCs are non-BMP4 responsive and weakly proliferative, I reasoned that combined inhibition of various receptor tyrosine kinases (RTKs) including VEGF receptor and PDGF receptor would promote naïve-like self-renewal. Sunitinib malate (in combination with LIF 3i or LIF-XAV-PD) was a robust addition to our minimal naïve cocktail. While it is mechanistically unclear at this stage why sunitinib malate promotes naïve-like growth in rhesus ESCs, global VEGF receptor inhibition may prove to be important for attaining a stable mouse ESC-like state in non-permissive PSC donors (including rhesus *and* human non-permissive PSC lines). Indeed, Chen et al. demonstrate that sunitinib malate alone promotes undifferentiated mouse ESC self-renewal in the absence of feeder cells or LIF, and such a '1i' cocktail without LIF supports mouse ESC self-renewal as successfully as classical Austin Smith LIF 2i<sup>72</sup>. Chen and colleagues further show that their 1i cocktail facilitates the *de novo* derivation of mouse ESCs from blastocysts that later contribute to chimeric mice<sup>72</sup>. Remarkably, they also show that 1  $\mu$ M sunitinib-containing medium facilitates the generation of iPSCs from mouse embryonic fibroblasts (MEFs) with only one factor (OCT4)<sup>72</sup>. Ultimately then, it will be valuable to further investigate a possible role for VEGF receptor inhibition in rhesus and human ground state self-renewal. On the human front, the potential of sunitinib to promote human naïve pluripotency has been

investigated by Jaenisch and colleagues and presented as supplemental data (see Theunissen et al. 2014). After engineering OCT4-2A-GFP reporter human ESC with a deletion of the OCT4 proximal enhancer ( $\Delta$ PE), Theunissen et al. identify OCT4- $\Delta$ PE-GFP<sup>+</sup> cells with sunitinib during their high-throughput kinase inhibitor screen to identify small molecules that promote naïve human pluripotency<sup>25</sup>. While they do not incorporate sunitinib into their cocktail of 5i/L/A (MEKi, GSK3 $\beta$ i, ROCKi, BRAFi, LCK/SRCi<sup>90</sup>, hLIF, Activin A), sunitinib malate was strongly identified during their screen for inhibitors that support human naïve pluripotency. After doxycycline-withdrawal of KLF2 and NANOG transgene expression in their engineered reporter lines, they identify SU11248 (sunitinib) on top of LIF 2i plus the BRAF inhibitor SB590885<sup>25</sup>. While it seems that BRAF inhibition synergizes with LIF 2i/sunitinib to produce human OCT4- $\Delta$ PE-GFP<sup>+</sup> cells (LIF 2i/sunitinib alone does not produce OCT4- $\Delta$ PE-GFP<sup>+</sup> cells<sup>25</sup>), the use of XAV939 may synergistically replace BRAF inhibition for the better in our attempt to induce rhesus naïve pluripotency. Indeed, XAV939 and sunitinib (together with LIF 2i) may prove useful for human naïve pluripotency.

Mechanistically, why might VEGF receptor inhibition promote mouse ESC-like self-renewal in rhesus ESCs? Presumably, the stress of single cell dissociation in combination with hypoxia stimulates the secretion of vascular endothelial growth factor (VEGF) molecules into the immediate *in vitro* culture environment. This is likely to occur via activation of an endoplasmic reticulum (ER) stress/HIF-1 $\alpha$  signalling axis<sup>72</sup>. Indeed, I suspect that this is the reason for notable spontaneous differentiation seen in ORMES-22 primed cultures grown with hypoxia. While evidence suggests that hypoxia may be beneficial for the undifferentiated propagation

of rESC<sup>69,91</sup> and human ESC cultures<sup>92</sup>, other groups have reported vascular-lineage priming of mouse ESCs with hypoxia (via HIF1-dependent mechanisms)<sup>93,94</sup>. In this regard, hypoxia may act somewhat like a double-edged sword: it may simultaneously promote  $\beta$ -catenin activation and enhance the self-renewal of PSCs<sup>95</sup>, but also may act to induce discreet vascular-lineage differentiation. Here, inhibiting VEGF receptor (in particular) with sunitinib malate may not only suppress stress/hypoxia induced differentiation, but fortify the combined effect of LIF 2i for the following two reasons: (1) LIF/LIF receptor/gp130 activation has a secondary effect of supposedly inhibiting HIF-1 $\alpha$ /ER stress activation and subsequent secretion of VEGF<sup>72,96</sup>; and (2) GSK-3 $\beta$  and MEK/ERK lie downstream of VEGF/VEGF receptor activation to reinforce the effect of CHIR99021 and PD0325901 (**Figure 14**).

To investigate whether the naïve cocktail of LIF 5i is dispensable for naïve rhesus reversion, fresh primed rESCs were converted with six chemical combinations of LIF, CHIR, PD, XAV, and SU (under both normoxic and hypoxic conditions). Surprisingly, the condition of normoxic LIF CHIR-PD-SU provided the greatest growth rates, but unfortunately, this condition appeared to differentiate the converted cells. While the normoxic condition of LIF XAV-PD-SU showed moderate growth kinetics, SSEA-4 expression as assessed via live staining was robust. Given that hypoxia promotes murine autocrine VEGF signalling<sup>72</sup>, it appears that SU effectively does not have to work as much against VEGF ligands under normoxic conditions and therefore has a greater effect without hypoxia. While hypoxia stimulates active  $\beta$ -catenin in pluripotent stem cells<sup>95</sup> and promotes stem/progenitor cell enrichment<sup>97</sup>, it may have secondary undesirable consequences for naïve (or primed) rhesus growth. In fact, I am currently examining whether addition of a blocking antibody to VEGF

receptor 2 can prevent the typical spontaneous differentiation seen in primed ORMES-22 rESCs. If selectively blocking VEGF receptor 2 maintains hypoxic primed ORMES-22 cells in a prolonged undifferentiated state, it may indicate that indeed hypoxia promotes VEGF secretion in rESCs. In support of hypoxia promoting active  $\beta$ -catenin, conversion of ORMES-22 rESCs with hypoxia did seem to buffer all six chemical conditions towards a similar growth trajectory compared to normoxia (**Figure 10E**), indicating the intrinsic potential of hypoxia to promote PSC self-renewal. However, hypoxic conversion for the ORMES-22 line appears to promote differentiation by passage 2 for most chemical combinations of inhibitors tested (**Figure 10B, C, D**).

Lastly, conversion of alternative CRES-2 SCNT and rPESC lines did not result in more efficient growth kinetics or SSEA-4 retention compared to the ORMES-22 line. It is likely that high-quality, transiently undifferentiated, primed cells are required for effective conversion efficiencies for these two alternative rhesus lines.

### **Examination of characteristic hallmarks for ground state pluripotency in LIF-3i converted human PSCs**

In order to further validate that LIF 3i converted “permissive” human iPSCs were classically naïve, further hallmarks of the naïve state were investigated. While the DNA methylation profile seen across the OCT4 distal enhancer was consistent with the naïve state, the OCT4 proximal enhancer methylation profile was inconclusive. However, LIF 3i human naïve PSCs displayed a statistically significant upregulation of homologous recombination (HR) genes (as assessed by GSEA) compared to their primed source counterparts. This is an exciting result for future gene targeting

experiments. Plasmid-based gene editing via HR may be greatly improved in the naïve state. Additionally, since current genome editing technologies creating synthetic double-strand breaks (i.e. ZFNs, TALENs, and CRISPR/Cas9 nucleases) *also* employ endogenous HR machinery to create sequence-specific edits with a donor vector, if these technologies were employed using the naïve pluripotent platform, gene targeting efficiencies could be significantly magnified (consider that HR-only mouse-ESC efficiencies are on the order of 20%). The upregulation of HR machinery genes could be beneficial for isogenic gene targeting as well, and it is likely that only one arm of a targeting vector would need to be sequence matched/PCR amplified from genomic DNA of host cells to result in an efficient biallelic genome editing event. Correction of sickle cell anemia and beta thalassemia mutations in patient-specific naïve iPSCs using the seamless genome-editing advantage of the PiggyBac transposon<sup>98–102</sup> is a useful proof-of-concept experiment likely set to validate the translational benefits of naïve PSCs.



## CONCLUSIONS AND PERSPECTIVES

Interrogation of naïve PSC self-renewal has shed tremendous light on a previously enigmatic state. Large-scale computational syntheses of ChIP-seq and microarray data has uncovered core transcription factor interactions in the ground state<sup>103</sup> and a computational synthesis of transcriptome data has revealed the validity of various naïve culture cocktails<sup>104</sup>; in essence, confirming our improved progress towards understanding the naïve ground state. Once further evidence accumulates that naïve PSCs possess improved differentiation potencies and enhanced amenability to plasmid-based HR over their primed counterparts, naïve pluripotent cell biology will be at the forefront of regenerative medicine. Beyond *in vitro* systems, blastocyst complementation experiments represent the most powerful application of ground state non-human primate and human PSCs. It is remarkable that via simple signaling inhibition and cytokine stimulation PSCs can be arrested in an ICM-like fate *in vitro*; it highlights that biological states once enigmatic, can be controllable after extensive and systematic mechanistic investigations. With each new study, it is evident that the methodological impact of naïve PSCs in stem cell biology and regenerative medicine will endure indefinitely.

## **MATERIALS AND METHODS**

### **Culture of mouse embryonic fibroblasts (MEFs)**

MEF cells at passage 2 were cultured for one week in two 0.1 % gelatinized T175 flasks, trypsinized (TrypLE Select, Gibco), counted, and split into ten T175 flasks for expansion at passage 3. MEF medium included: ~90% DMEM (Invitrogen) supplemented with ~10% FBS, 0.1 mM MEM non-essential amino acids (Gibco), L-glutamine to a final concentration of 2mM (Gibco), 0.1 mM  $\beta$ -mercaptoethanol (Sigma) and penicillin/streptomycin (Gibco). Cells were harvested and irradiated for mitotic inactivation at 5000 rad. Cells not needed immediately were cryopreserved.

### **Culture of primed rhesus monkey embryonic stem cells (rESCs)**

All primed pluripotent stem cell lines used in this study were co-cultured on irradiated DR4 MEF feeders and incubated under hypoxic conditions at 37°C, 5% CO<sub>2</sub> and 85% relative humidity (unless otherwise indicated). Cells were fed daily and maintained with regular hESC medium consisting of ~80% DMEM/F12 (Invitrogen) medium supplemented with ~20% Knockout Serum Replacement (KOSR; Invitrogen), 0.1 mM MEM non-essential amino acids (Gibco), L-glutamine to a final concentration of 1mM (Gibco), 0.1 mM  $\beta$ -mercaptoethanol (Sigma) and FGF2 to a final concentration of 20 ng/mL (R&D systems). Cells were both manually passaged (using a pipette above an inverted microscope to manually detach and select hESCs colonies with good morphology -- sharp edges, homogenous interior, shiny non-dark surface) and passaged in bulk using a cell scraper to detach pluripotent stem cells. Both protocols involved a 5min collagenase digestion at 37°C to loosen colonies prior to detachment.

### **Culture of naïve rhesus monkey embryonic stem cells (rESCs)**

“Naïve” culture conditions for ground-state pluripotency included the addition of various cytokines and small molecule inhibitors. Cells were alternatively cultured under normoxia or hypoxia with DR4 MEF feeders and fed daily (to compensate for the short half-life of small molecules employed). All naïve formulations consisted of basal KOSR-based hESC medium without bFGF (unless otherwise indicated). The following cytokines and small molecules (with optimal working concentrations) were used in various combinations throughout this study: human LIF (20ng/mL, alternatively purchased from Sigma, cat no. L5283, Cell Signaling, cat no. 8911LC, or Peprotech, cat no. 300-05), PD0325901 (1 $\mu$ M, Stemgent, cat no. 040006 or Sigma, cat no. PZ0162), CHIR99021 (3 $\mu$ M, Stemgent, cat no. 04-0004 or Tocris Bioscience, cat no. 4423), XAV939 (4 $\mu$ M, Sigma, cat no. X3004), Forskolin (10 $\mu$ M, Stemgent, cat no. 04-0025), Purmorphamine (2 $\mu$ M, Stemgent, cat no. 04-0009), Sunitinib malate (1 $\mu$ M, Sigma, cat no. PZ0012), lithium chloride (10mM, Sigma, cat no. 298328), and BMP4 (10ng/mL, Peprotech). Additionally, where indicated, ROCK inhibitor was also used at 10 $\mu$ M (Stemolecule Y27632, Stemgent, cat no. 04-0012). Conversion of primed bFGF lines consisted of a 48-hour adaptation step followed by single cell dissociation using StemPro Accutase cell detachment solution (Life Technologies). Single cells were re-plated at densities between 50,000 to 100,000 cells/cm<sup>2</sup>. All cell cultures were counted with a Countess Cell Counter (Life Technologies) via trypan blue exclusion. Cultures were examined with phase contrast microscopy using an Eclipse TE-2000 inverted microscope (Nikon Instruments) equipped with a DS-Fi1 camera and NIS-Elements software (Nikon Instruments). Note: conventional LIF 3i consists of human LIF, plus three small molecule inhibitors: CHIR99021 (GSK3 $\beta$ i),

PD0325901 (MEK/ERKi), and XAV939 (WNT modulator). LIF 5i consists of LIF 3i plus forskolin and purmorphamine.

**Monitoring phenotypic pluripotency (flow cytometry, alkaline phosphatase staining, and live fluorescent staining)**

Retention of phenotypic pluripotency was measured by flow cytometry using anti-human SSEA-4 (R&D) and TRA-1-81 (BD-Biosciences) antibodies. Primed and naïve cultures were briefly washed once in phosphate-buffered saline (PBS, Life Technologies) and dissociated using Accutase solution for 5 min at 37°C. After enzymatic neutralization, single cell suspensions were re-suspended in culture medium and counted using a Countess Cell Counter. After one wash in PBS, 100,000 - 200,000 cell aliquots were incubated for 20 minutes at 4°C with monoclonal mouse antihuman antibodies SSEA4-APC (5µL, cat no. FAB1435A, R&D Systems) and TRA-1-81-PE (10µL, cat no. 560161, BD-Biosciences). Isotype controls matching each immunoglobulin subtype were stained analogously to measure non-specific binding. To quantitatively measure SSEA-4<sup>+</sup> or TRA-1-81<sup>+</sup> cells, exactly 10,000 events per sample (at a rate below 300 events per second) were acquired using a dual laser FACSCalibur flow cytometer (BD-Biosciences) equipped with blue argon (488 nm) and red diode (635 nm) lasers and the BD CellQuest Pro analytical software (BD-Biosciences). Analysis was conducted using FlowJo single cell FACS software (Tree Star).

To conduct alkaline phosphatase staining, cultures were gently fixed in 2% PBS/paraformaldehyde (Affymetrix) for 10 minutes, washed with PBS, and stained with BCIP/NBT substrate (Life Technologies) for 10-15 min at room temperature.

Reactions were stopped after 15 minutes and wells were subsequently washed twice with PBS and imaged.

Lastly, live staining for SSEA-4 expression was conducted using a mouse anti-human SSEA-4 NL493-conjugated monoclonal antibody. Live cells were stained for 2 hours using 1x SSEA-4 NL493 antibody in cell culture medium and subsequently washed once with cell culture medium and once with PBS. The cells were examined using epifluorescence in 1x Live Cell Imaging Solution (Life Technologies).

### **GSEA and Infinium DNA methylation array analysis**

KEGG (Kyoto Encyclopedia of Genes and Genomes) gene sets for homologous recombination (HR) and non-homologous end joining (NHEJ) were used for gene set enrichment analysis (GSEA). Normalized Illumina arrays from human LIF 3i naïve and bFGF source cell lines were probed for differences in HR or NHEJ pathway genes using online GSEA software (<http://www.broadinstitute.org/gsea/index.jsp>). To examine the DNA methylation profile across the human OCT4 proximal and distal enhancers, Infinium 450k methylation array data from human LIF 3i naïve and bFGF source lines was kindly provided by JH. Using sequence homology to luciferase vectors from Gafni et al.<sup>21</sup>, the human coordinates for the proximal and distal enhancers were extracted and aligned to CpG probes from the 450k methylation array. To locate probes within the enhancers, SnapGene software was used for sequence examination. Beta values at each probe were subsequently plotted using GraphPad Prism software.

## FIGURES

**Figure 1**

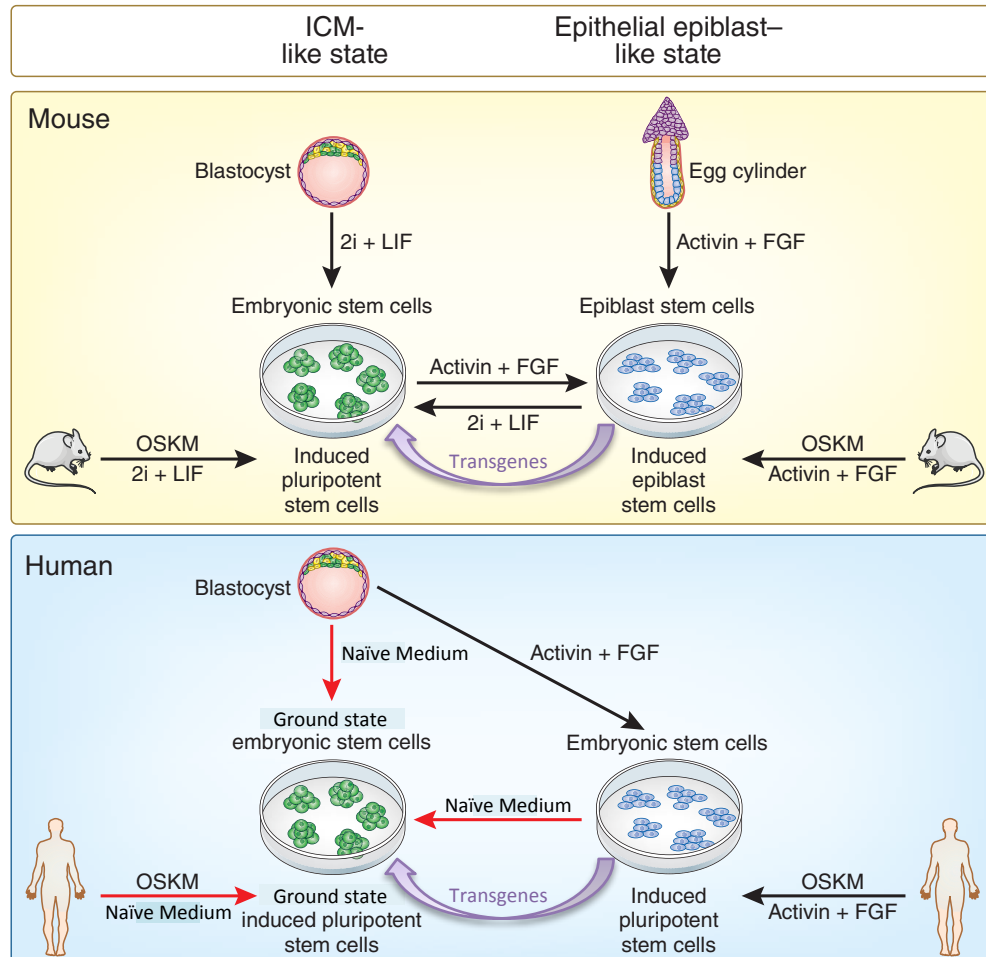


**Figure 1: Species-specific contextual examination of naïve pluripotency between mice and humans**

In mice, epiblast stem cells corresponding to the egg cylinder stage of development depend on Activin and FGF signaling, while embryonic stem cells corresponding to the inner cell mass (ICM) of the blastocyst depend on LIF/STAT signaling (with 2i). Derivations from somatic cells, blastocysts, and egg cylinders are depicted, together with the reversible interconversion between primed and ground state pluripotency (via

transgene-free methods or transgene-dependent methods). Like in mice, ground state human embryonic stem cells may be isolated from the ICM when cultured in LIF/STAT-conductive media (with further signaling inhibitors), or primed cells may be isolated when cultured with Activin and FGF. Derivations from somatic cells and blastocysts are depicted, together with the interconversion between primed and ground state pluripotency (via transgene-free methods or transgene-dependent methods). Naïve medium refers to human embryonic stem cell medium supplemented with human LIF, MEK/ERK inhibition, GSK3 $\beta$  inhibition, and various other small molecule inhibitors and recombinant growth factors. Notably, work by Zimmerlin et al. only requires the addition of axin-stabilizing XAV939 above basal LIF 2i medium to convert primed human PSCs into ground state PSCs. Abbreviations: OSKM = OCT4, SOX2, KLF4, and c-MYC (the Yamanaka factors<sup>105</sup>). This figure is modified from Mascetti & Pedersen (2014)<sup>2</sup>.

**Figure 2**

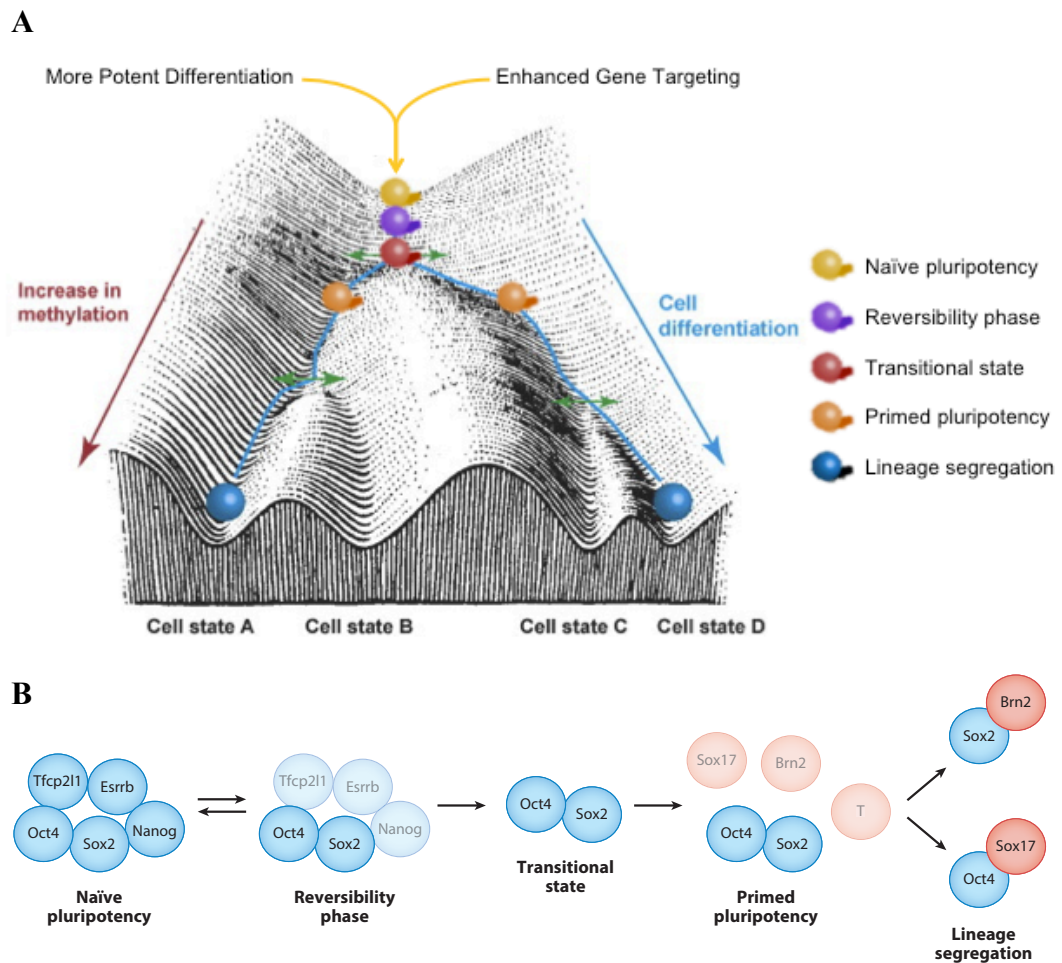


**Figure 2: The changing epigenetic and transcription factor landscape seen across the transition from naïve pluripotency to primed pluripotency**

(A) The transition through various stages of stem cell potency: naïve pluripotency; a reversibility phase; a transitional state; primed pluripotency, and finally lineage segregation. The stages of stem cell potency are depicted along Waddington's Epigenetic Landscape, first proposed by C. H. Waddington in 1942. Waddington's Landscape classically depicts the process of differentiation as a fall in "potential energy" (so to speak) and an increase in DNA methylation. Notice

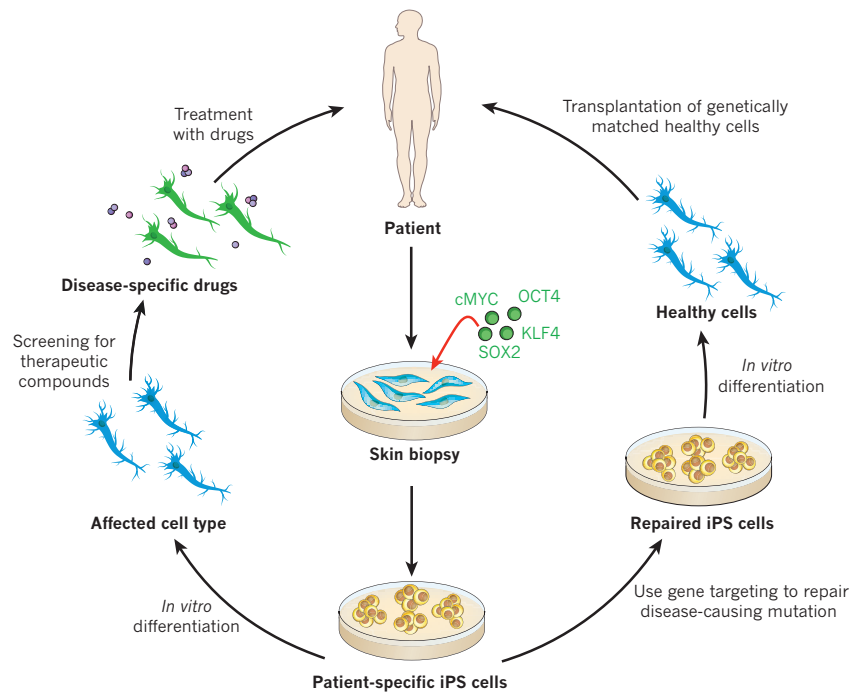


that the naïve pluripotent cell is globally demethylated compared to the primed pluripotent cell. The open chromatin landscape of the naïve cell compared to the primed cell confers two advantageous properties for *in vitro* stem cell biology: more potent differentiation capabilities and enhanced gene targeting via plasmid-based homologous recombination. Modified from Barth and Imhof (2010)<sup>106</sup>.

**(B)** The stages of stem cell potency described in (A) are depicted here with a focus on the key transcription factor circuits involved in maintaining a particular cell fate. The progression from ground state naïve pluripotency to lineage commitment involves a gradual loss in naïve factors (light blue). The first transition is initially reversible until naïve factors (Tfcp2l1, Esrrb, Nanog) are gradually lost in the transitional state. In response to external signals (such as FGF, Nodal, and Wnt), cells in the transitional stage upregulate lineage markers (such as Sox17, Brn2, and T) on their way to primed pluripotency. Primed pluripotent cells are then free to enter definitive lineages. Shown here are neuroectodermal (Sox2 and Brn2 positive) and mesendodermal (Oct4 and Sox17 positive) progenitors. Used unmodified from Martello and Smith (2014)<sup>107</sup>.

**Figure 3**

**A**



**B**

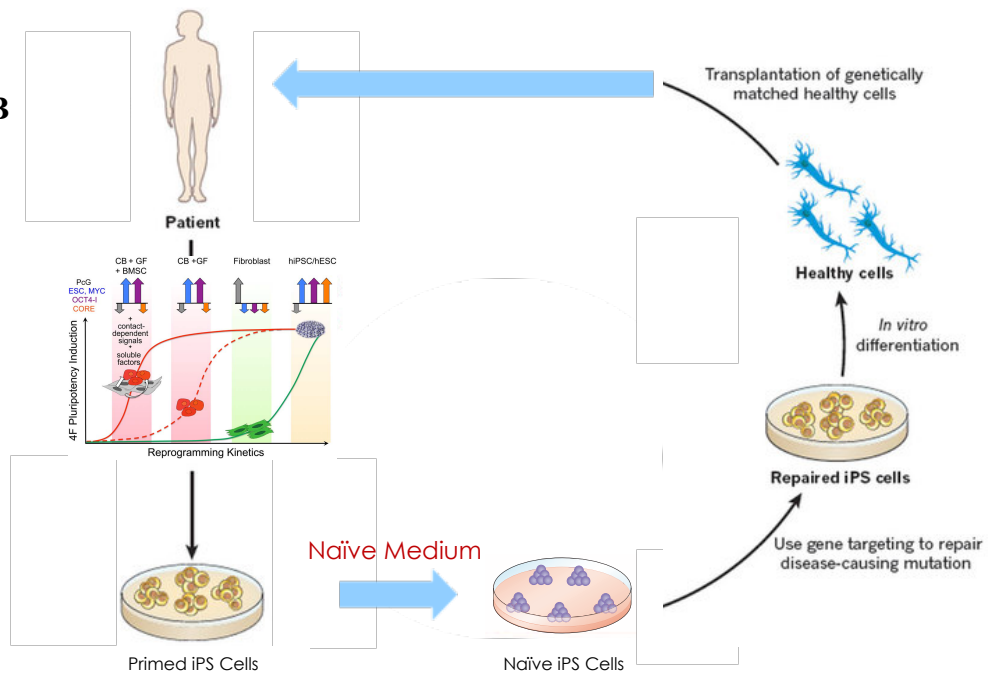


**Figure 3: Naïve pluripotency revises the clinical iPS paradigm**

(A) The clinical paradigm of iPS reprogramming technology. Here, patient-specific iPS cells generated from skin biopsy cells via ectopic co-expression of the

Yamanaka factors (OCT4, SOX2, KLF4, and c-MYC) can be used for *in vitro* differentiation and personalized drug screening (left path); or can be used to correct an inherited mutational disorder *in vitro* via powerful genome editing technologies and subsequently re-differentiated into desired lineages for transplantation therapy (right path). The benefit of using iPS cells here is that these cells are always genetically matched to a specific patient (the patient provides the somatic cells prior to reprogramming). Used unmodified from Robinton and Daley (2012)<sup>108</sup>.

**(B)** Naïve pluripotency reshapes the canonical iPS cell paradigm presented in (A). As Zimmerlin et al. (2015) argue, by combining the utility of high fidelity optimized reprogramming to pluripotency together with naïve reversion, we may create new opportunities for gene repair and *in vitro* directed differentiation to operate with clinically relevant efficiencies and kinetics. Note that the path begins with a graphic depicting stromal-primed reprogramming of myeloid progenitors<sup>109</sup>. Modified from Robinton and Daley (2012)<sup>108</sup> and Park et al. (2012)<sup>109</sup>.

**Figure 4**

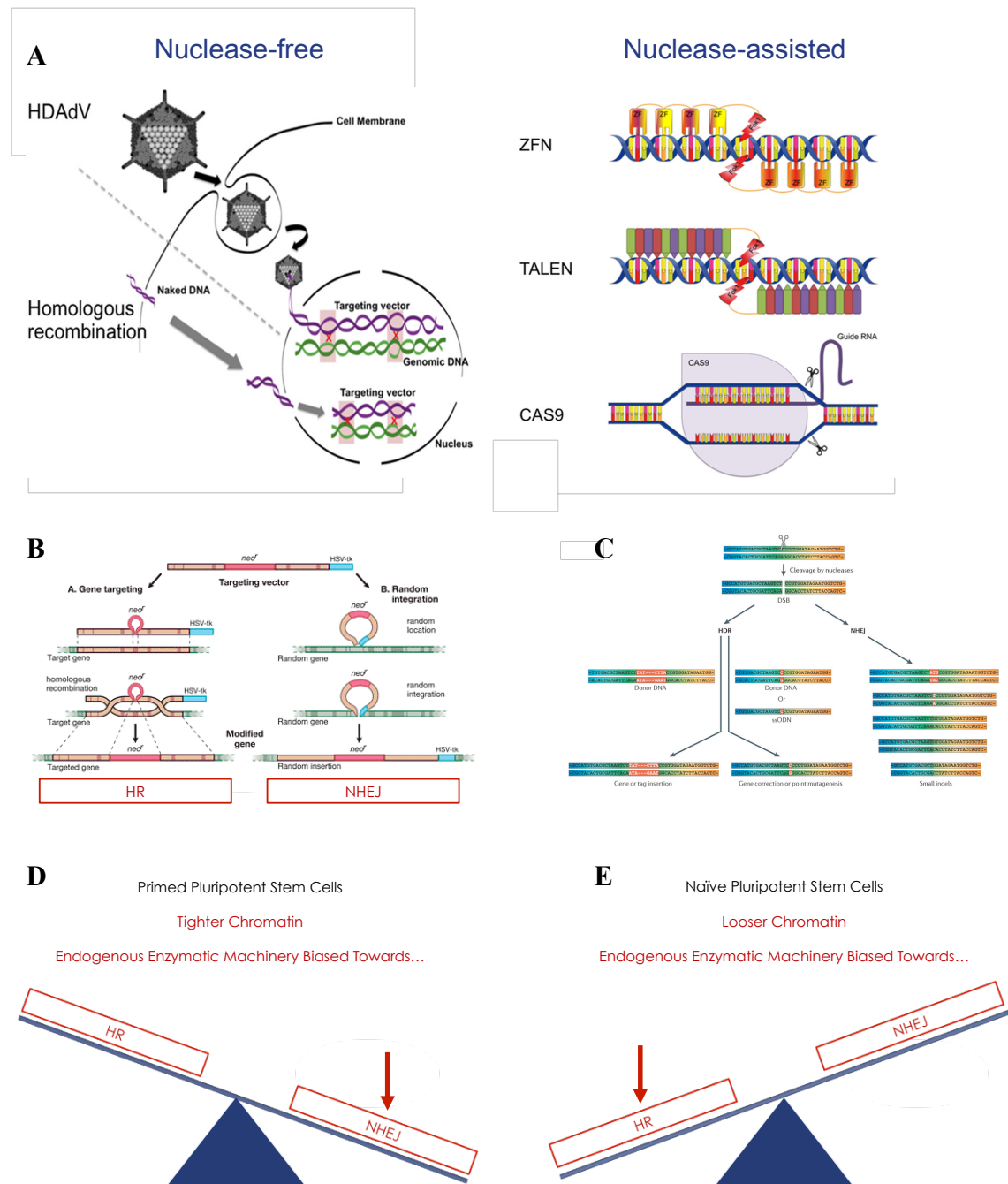


**Figure 4: Genome editing technologies and the ground state advantage**

(A) The current genome editing toolbox. Five technologies exist to gene target pluripotent stem cells. Of the five, two are nuclease-free: (1) helper-dependent adenoviral vectors (HDAdVs) packaged with gene targeting vectors; and (2)

direct plasmid-based homologous recombination. The remaining three are nuclease-assisted and derived primarily to overcome the weak homologous recombination capacity of primed pluripotent stem cells. These technologies simply create synthetic double-strand breaks (DSBs) in DNA and require the co-transfection of donor sequences to mediate sequence-specific edits via endogenous HR. These include: (1) zinc-finger nucleases (ZFNs); (2) transcription activator-like effector nucleases (TALENs); and (3) clustered regularly interspaced short palindromic repeat - associated nuclease 9 (CRISPR-Cas9) technology. Modified from Li et al. (2014)<sup>49</sup>.

**(B)** Of the technologies presented in (A), the nuclease-free technologies make sequence-specific edits in the genome via two endogenous, and competing, DSB-repair pathways: homologous recombination (HR) and non-homologous end joining (NHEJ). Shown here are targeting vectors with two homology arms and neomycin drug-resistance being integrated into the genome in a sequence-specific manner via HR (targeted integration) or randomly via NHEJ (random integration). Primed cells have greater capacity for NHEJ and therefore require the assistance of synthetic DSBs to mediate correct sequence-specific targeting. Modified from Nobelprize.org<sup>110</sup>.

**(C)** When synthetic-nucleases are used to mediate gene targeting, DSBs in DNA can lead to sequence-specific insertions or corrections (red box) via homology-directed repair (HDR) in the presence of a double-stranded donor template or single-stranded oligodeoxynucleotide (ssODN), each of which contain homology arms. The induced DSBs can also be repaired via error-prone NHEJ, which does

not require any template sequence and therefore can lead to mutational insertions and deletions (indels). Modified from Kim and Kim (2014)<sup>111</sup>.

**(D)** Primed pluripotent cells are globally hypermethylated relative to naïve cells and therefore possess a tighter chromatin landscape. Additionally, endogenous enzymatic machinery in the primed background favors error-prone NHEJ (which mediates random integration of plasmid-based gene targeting vectors).

**(E)** Naïve pluripotent cells are globally hypomethylated relative to naïve cells and therefore possess a more open chromatin landscape. Endogenous enzymatic machinery in the naïve background favors HR (which mediates targeted integration of plasmid-based gene targeting vectors).

**Figure 5**

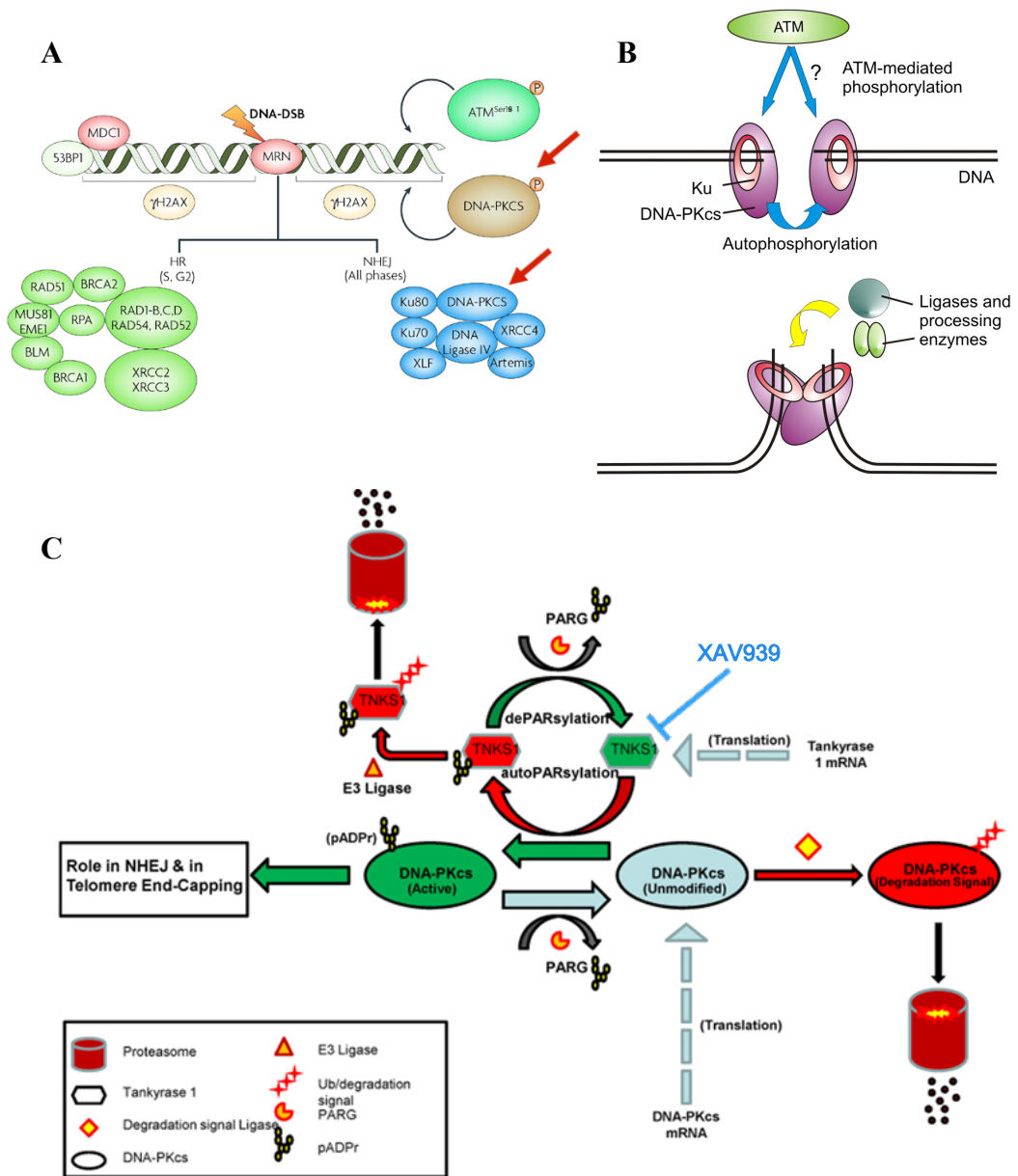


**Figure 5: NHEJ and the indirect depletion of DNA-PKCS by XAV939**

(A) Under normoxia, DNA DSBs are sensed by the MRE11–RAD50–NBS1 complex, leading to recruitment and activation of DNA-dependent protein kinase (DNA-PK) catalytic subunit (DNA-PKCS) and ataxia telangiectasia mutated (ATM). The histone variant H2AX ( $\gamma$ H2AX, yellow) is also phosphorylated at

the DSB. Subsequently, a number of DNA damage-sensing proteins such as p53-binding protein 1 (53BP1) and mediator of DNA damage checkpoint 1 (MDC1) are recruited for use in HR and NHEJ. HR molecules are indicated in light green and NHEJ molecules are indicated in blue. Red arrows indicate DNA-PKCS molecules. Modified from Bristow and Hill (2008)<sup>52</sup>.

**(B)** As part of the initial phases of NHEJ, a Ku70/80 heterodimer, together with DNA-PKCS, associate at the site of a DSB to protect against premature ligation and degradation of DNA termini. Trans auto-phosphorylation of DNA-PKCS induces a conformational change in the DNA-PKCS/Ku70/80 complex to make DNA termini more accessible for other NHEJ ligases and processing enzymes. ATM-mediated DNA-PKCS phosphorylation (together with trans auto-phosphorylation) may play a role in this conformational change. Modified from Weterings and Chen (2008)<sup>53</sup>.

**(C)** XAV939 is shown to target TNKS1, which relies on poly(ADP-ribose) glycohydrolase (PARG) activity to remove an auto-poly(ADP-ribose) group (auto-pADPr) to remain in an active state (green); otherwise, the enzyme is ubiquitinated in an inactive state (red) and targeted for proteasome-mediated degradation. In an active state, TNKS1 PARsylates unmodified DNA-PKCS (green arrow). This modification can be reversed via PARG activity (light blue arrow). After TNKS1 has PARsylated DNA-PKCS, it is auto-PARSylated (inactive red) and targeted for proteasome-mediated degradation. PARsylated DNA-PKCS are active and free to act in NHEJ repair of DNA DSBs; however, if DNA-PKCS is not PARsylated by TNKS1, it is marked for subsequent



proteasome-mediated degradation (right of schematic). If the PARP catalytic activity of TNKS1 is depleted or inhibited (here by XAV939), DNA-PKCS accumulates in its unmodified form and is forced towards proteasome-mediated depletion. Note that translation of DNA-PKCS mRNA renews the unmodified DNA-PKCS population, while translation of TNKS1 mRNA renews the active TNKS1 population. Modified from Dregalla et al. (2010)<sup>54</sup>.

**Figure 6**

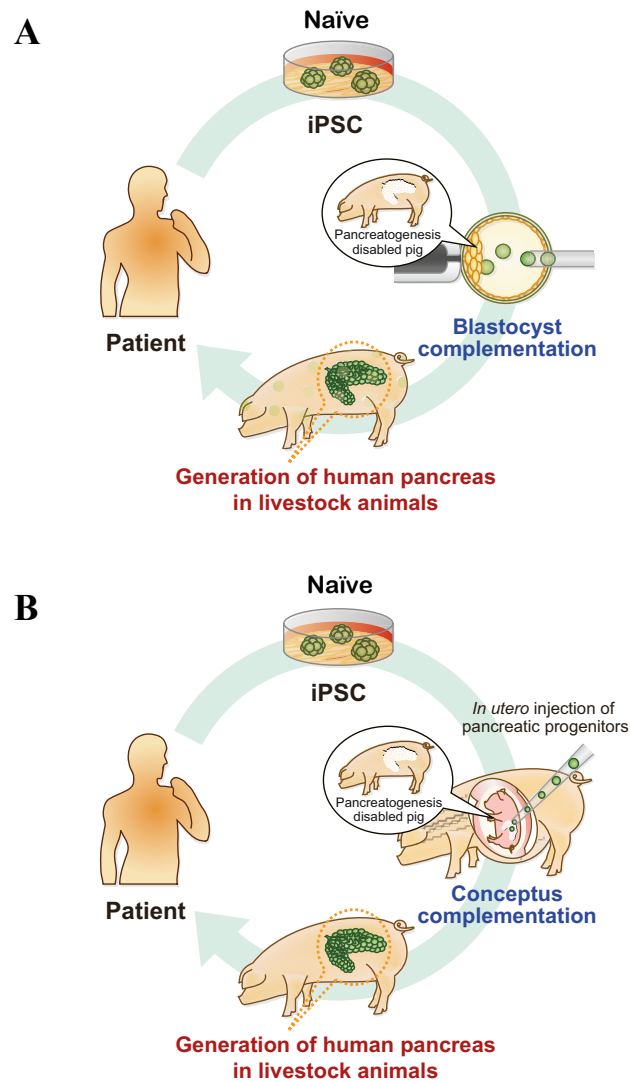


**Figure 6: Naïve pluripotency provides a future platform for the interspecies generation of human organs in livestock animals**

**(A)** The use of naïve patient-specific iPSC in blastocyst complementation with organogenesis-disabled livestock. Modified from Rashid et al. (2014)<sup>62</sup>.

**(B)** The use of naïve patient-specific iPSC in conceptus complementation *in utero* with organogenesis-disabled livestock. Modified from Rashid et al. (2014)<sup>62</sup>.

**Figure 7**

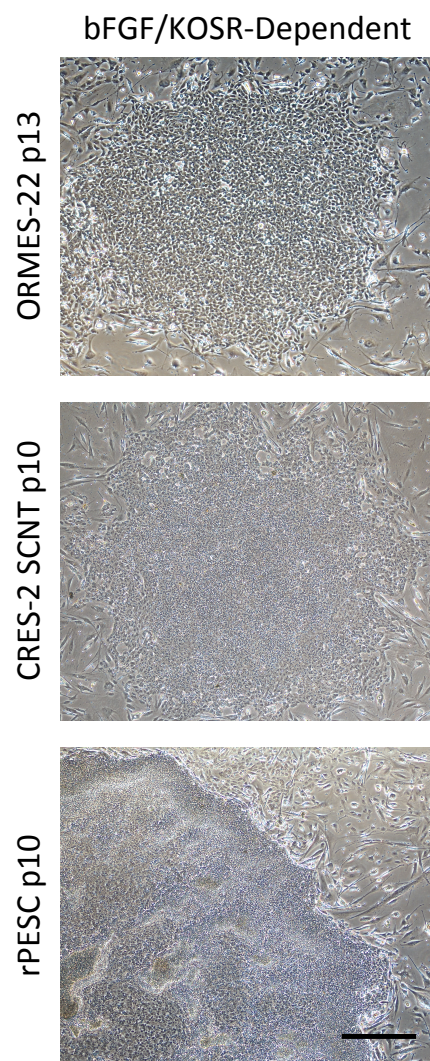


**Figure 7: Instability in primed bFGF/KOSR-dependent ORMES-22, CRES-2 SCNT, and rPESC lines**

Primed ORMES-22, CRES-2 somatic cell nuclear transfer (SCNT), and parthenogenetic rhesus ESC (rPESC) lines show instability when grown with basic fibroblast growth factor (bFGF) under basal hESC medium supplemented with 20% knockout serum replacement (KOSR). Primed cultures were imaged using phase contrast microscopy. Part of a colony is shown for rPESCs. Scale bar = 500  $\mu\text{m}$ .

**Figure 8**

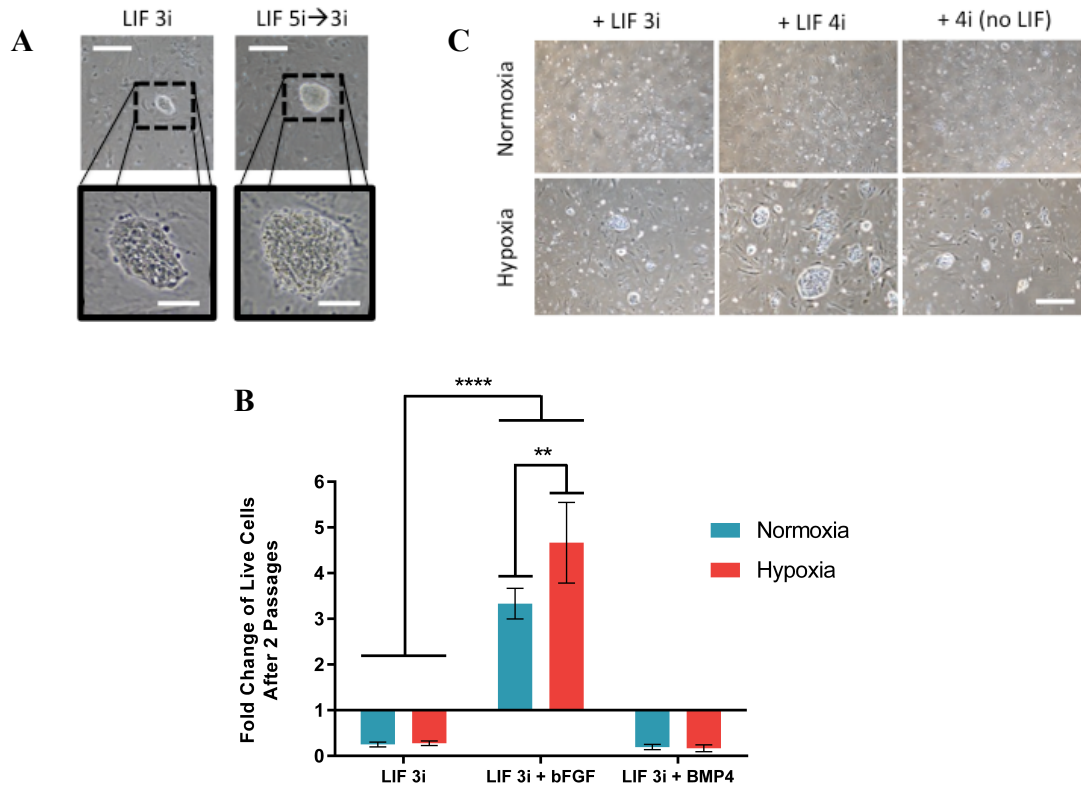


**Figure 8: Examination of naïve rhesus ESC domed-shaped morphology and clonal expansion post single cell passaging under different *in vitro* conditions**

**(A)** ORMES-22 p9 rhesus ESCs (rESCs) cultured in LIF 3i for 12 passages (left) and ORMES-22 p9 rESCs cultured in LIF 5i for 1 passage plus LIF 3i for 11 passages (right). Representative colonies are depicted. Phase contrast. Top panel, scale bar = 200  $\mu$ m; bottom panel, scale bar = 100  $\mu$ m.

**(B)** ORMES-22 p9 + 1 LIF 5i + 10 LIF 3i cells were cultured for two additional passages in either LIF 3i, LIF 3i supplemented with 20 ng/mL bFGF, or LIF 3i supplemented with 10 ng/mL BMP4 (under both normoxic and hypoxic conditions). Cell viability is depicted as measured by trypan blue exclusion. A 2-

way ANOVA was employed together with Sidak's multiple comparisons test in GraphPad Prism to assess statistical significance. \*\*\*\* =  $P \leq 0.0001$ ; \*\*  $P \leq 0.01$ .  $n = 3$  wells per condition; mean  $\pm$  SD indicated.

(C) ORMES-22 p9 rESCs cultured in LIF 5i for 1 passage, and LIF 3i for 11 passages were subjected to six different culture conditions. Representative colonies are depicted after 9-day treatment. Top panel: normoxia; bottom panel: hypoxia. Phase contrast. Scale bar = 200  $\mu\text{m}$ .

**Figure 9**

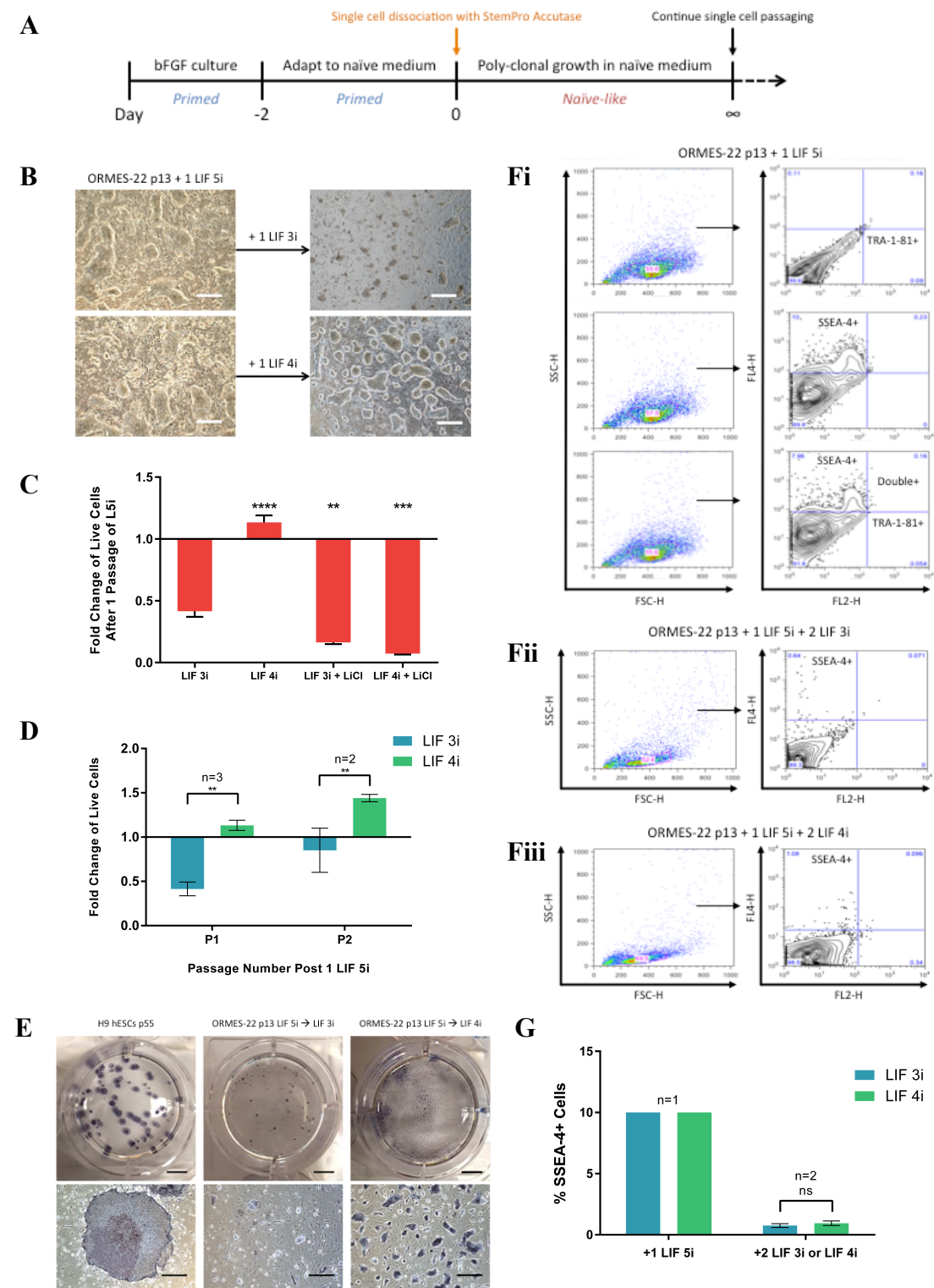


**Figure 9: Direct conversion of primed ORMES-22 p13 rESCs with one passage of LIF 5i and further passaging in LIF 3i or LIF 4i**

- (A) Protocol timeline depicting the conversion of primed pluripotent stem cells to poly-clonal naïve-like pluripotent stem cells. Conversion consists of three phases: regular bFGF primed culture, adaptation to naïve medium for 48 hours, and poly-clonal growth in naïve medium.
- (B) ORMES-22 p13 rESCs were converted with one passage of LIF 5i + 10 ng/mL bFGF (n = 3). Cells were then passaged into either LIF 3i or LIF 4i (consisting of LIF 3i + 1  $\mu$ M sunitinib). All cultures were incubated under hypoxic conditions. Phase contrast. Scale bar = 500  $\mu$ m.
- (C) ORMES-22 p13 + 1 LIF 5i rESCs were passaged into four different conditions: LIF 3i, LIF 3i + 1  $\mu$ M sunitinib, LIF 3i + 10 mM LiCl, and LIF 3i + 1  $\mu$ M sunitinib + 10 mM LiCl. Cell viability as measured by trypan blue exclusion was measured after one passage. An ordinary one-way ANOVA with Tukey's multiple comparisons test was employed in GraphPad Prism to assess statistical significance versus the L3i control. \*\*\*\* =  $P \leq 0.0001$ ; \*\*\* =  $P \leq 0.001$ ; \*\*  $P \leq 0.01$ . n = 3 wells per condition; mean  $\pm$  SD indicated.
- (D) ORMES-22 p13 + 1 LIF 5i cells were cultured for two additional passages in LIF 3i or LIF 4i under hypoxic conditions. Shown is the fold change in live cells per passage. A 2-way ANOVA was employed together with Tukey's multiple comparisons test in GraphPad Prism to assess statistical significance. \*\*  $P \leq 0.01$ .

- (E)** ORMES-22 p13 + 1 LIF 5i + 3 LIF 3i or 4i rESCs were stained with BCIP/NBT substrate for alkaline phosphatase expression. H9 human embryonic stem cells (hESCs) at passage 55 were used as a positive control. Scale bar (wells) = 1500  $\mu\text{m}$  and scale bar (phase contrast microscopy) = 500  $\mu\text{m}$ .
- (F)** **(i)** Flow cytometry was conducted on ORMES-22 p13 + 1 LIF 5i cells to detect pluripotency surface markers using TRA-1-81 PE-conjugated and SSEA-4 APC-conjugated antibodies (n = 1). Top panel = TRA-1-81 stained cells with positive quadrant indicated; middle panel = SSEA-4 stained cells with positive quadrant indicated; bottom panel = doubly stained cells with positive quadrant indicated. APC = allophycocyanin; PE = phycoerythrin; SSC-H = side scatter (granularity); FSC-H = forward scatter (size); FL2-H = PE channel; FL4-H = APC channel. The left column depicts the SSC-H x FSC-H plots of all 10, 000 events recorded per staining; the right column depicts viable cells that were manually gated from each left column plot per staining. All analysis was conducted using FlowJo software. **(ii)** ORMES-22 p13 + 1 LIF 5i + 2 LIF 3i rESCs stained for SSEA-4 (n = 2; representative data indicated). **(iii)** ORMES-22 p13 + 1 LIF 5i + 2 LIF 4i rESCs stained for SSEA-4 (n = 2; representative data indicated).
- (G)** Quantification from (E). A 2-way ANOVA with Sidak's multiple comparisons test was employed in GraphPad Prism to assess statistical significance.



Figure 10

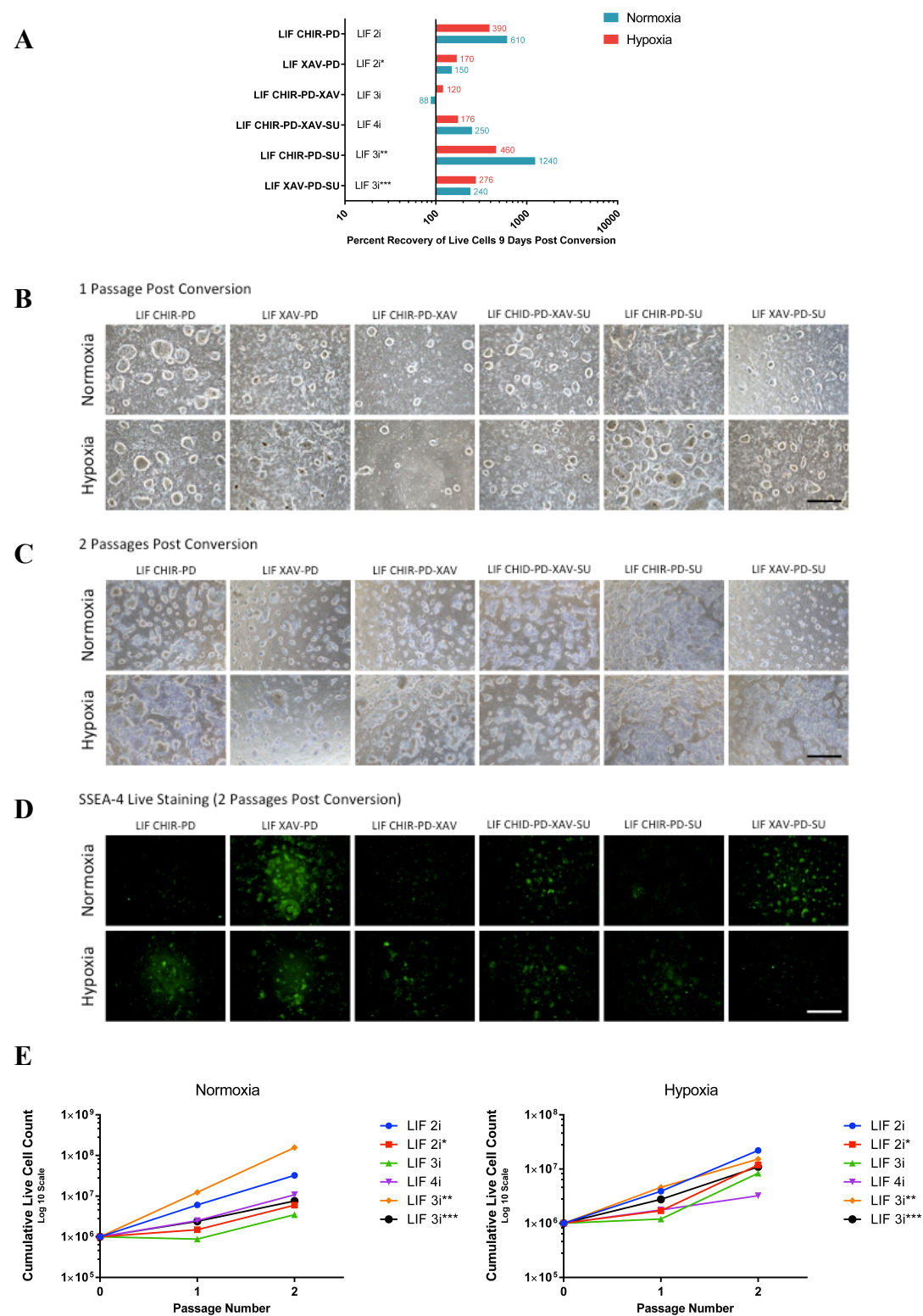


**Figure 10: Direct conversion of ORMES-22 rESCs with varied combinations of LIF, CHIR, PD, and SU**

- (A) ORMES-22 p19 rESCs were converted in the indicated conditions. Percentage recovery of live cells as measured by trypan blue exclusion was determined 9 days post single-cell dissociation.
- (B) Comparative examination of dome shaped morphology across the 12 different *in vitro* culture conditions indicated in (A) after one passage. Cells were imaged under phase contrast. Scale bar = 500  $\mu\text{m}$ .
- (C) Examination of morphology after two passages in the indicated conditions. Phase contrast; scale bar = 500  $\mu\text{m}$ .
- (D) The cells depicted after two passages were live stained for SSEA-4 (using a mouse anti-human monoclonal antibody conjugated to NL493). Cells were imaged using epifluorescence microscopy under blue light. Scale bar = 500  $\mu\text{m}$ .
- (E) Examination of growth kinetics across the 12 different conditions tested over two passages (6 conditions under normoxia and 6 conditions under hypoxia). Total live cells as measured by trypan blue exclusion was determined and plotted on a log<sub>10</sub> scale.

**Figure 11**

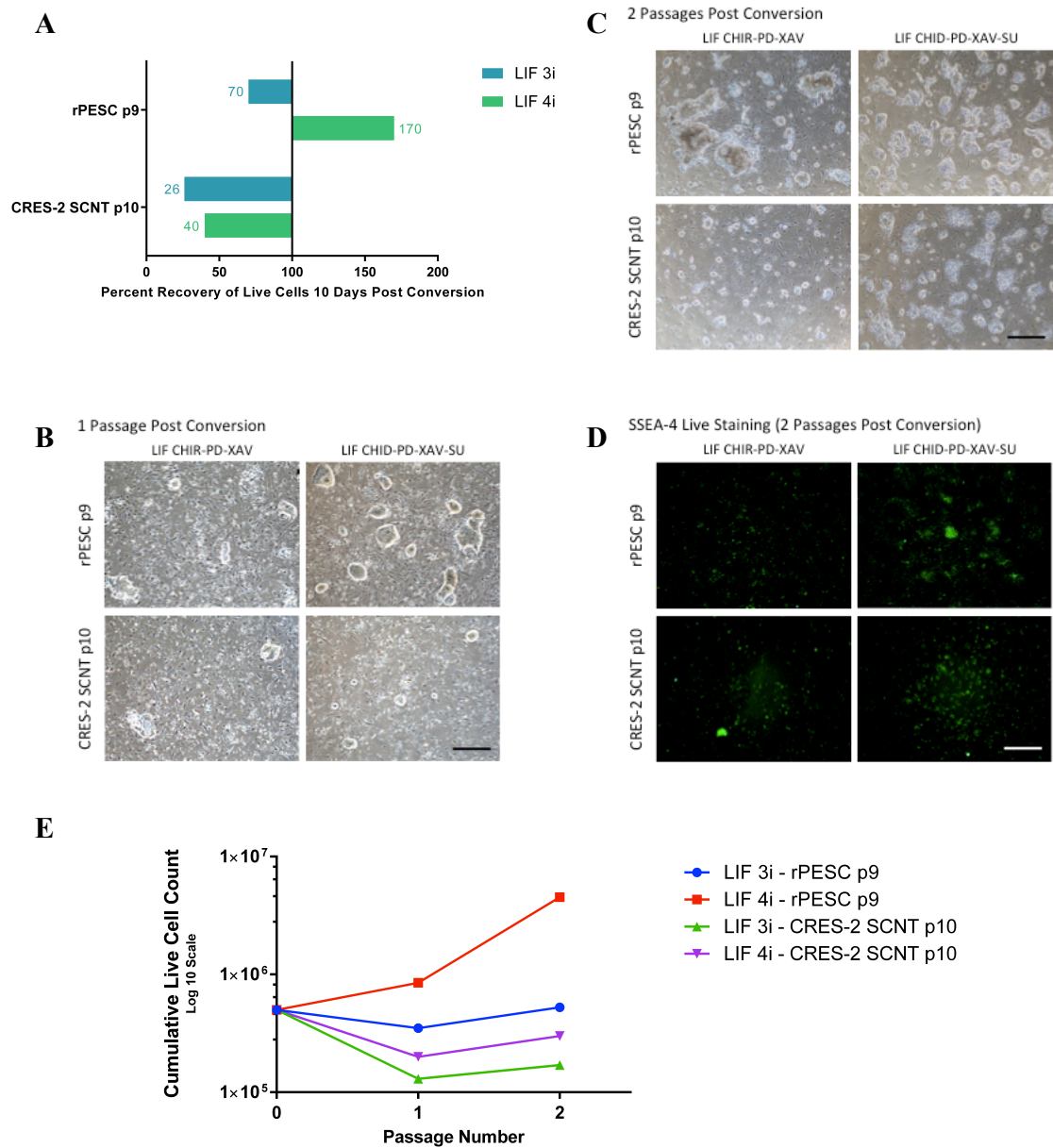


**Figure 11: Direct conversion of alternative rhesus macaque embryonic stem cell lines derived from SCNT (CRES-2) or parthenogenesis (rPESC)**

(A) Primed pluripotent cells were converted in the indicated conditions (LIF 3i or LIF 4i) under hypoxia only. Percentage recovery of live cells as measured by trypan blue exclusion was determined 10 days post single-cell dissociation.

- (B)** Comparative examination of dome shaped morphology across the different *in vitro* culture conditions indicated in (A) after one passage. Cells were imaged under phase contrast. Scale bar = 500  $\mu\text{m}$ .
- (C)** Examination of morphology after two passages in the indicated conditions. Phase contrast; scale bar = 500  $\mu\text{m}$ .
- (D)** The cells depicted after two passages were live stained for SSEA-4 (using a mouse anti-human monoclonal antibody conjugated to NL493). Cells were imaged using epifluorescence microscopy under blue light. Scale bar = 500  $\mu\text{m}$ .
- (E)** Examination of growth kinetics across the 2 different conditions tested over two passages. Total live cells as measured by trypan blue exclusion was determined and plotted on a log<sub>10</sub> scale.

**Figure 12**

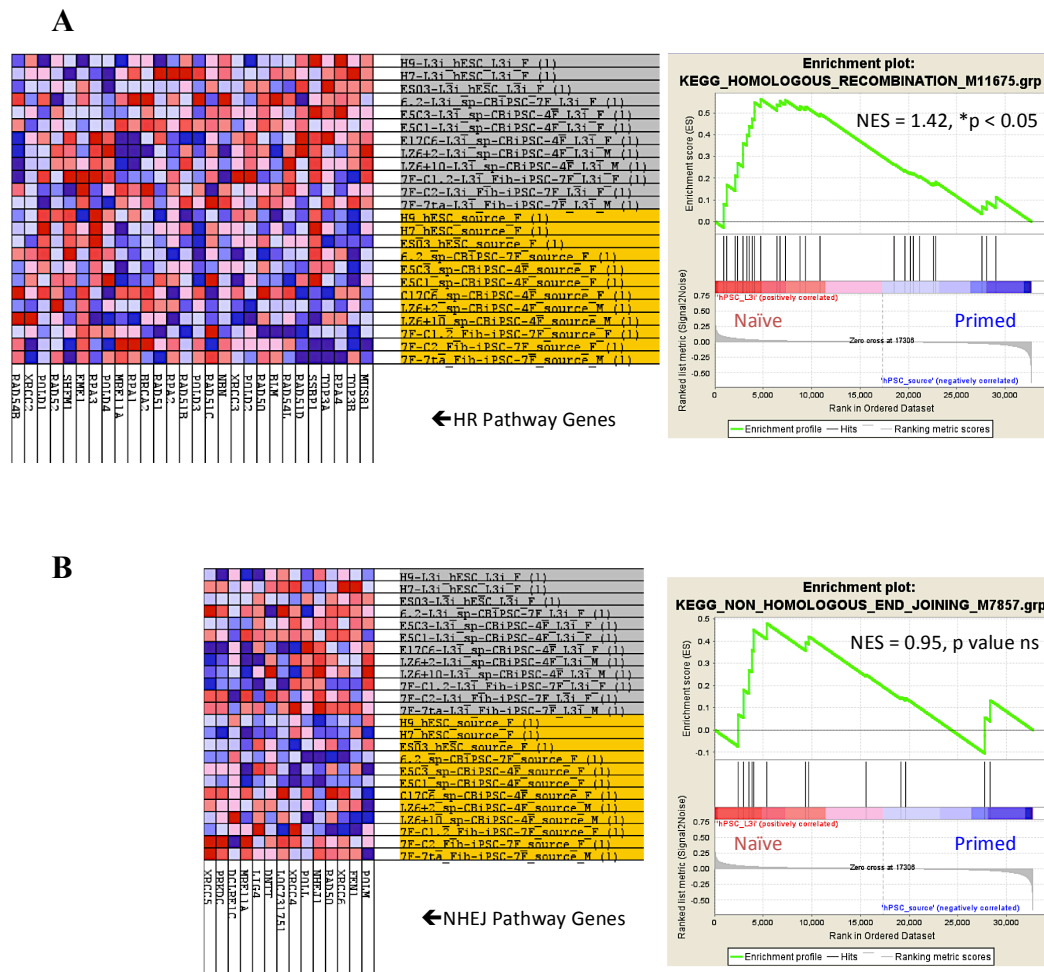


**Figure 12: LIF 3i converted human pluripotent stem cells display significant enrichment in HR pathway genes**

Gene set enrichment analysis for **(A)** homologous recombination (HR) and **(B)** non-homologous end joining (NHEJ) pathways of double-strand break DNA repair. NES = normalized enrichment score, ns = not significant. Each column on the heatmaps represents a different gene (indicated below each heatmap). The corresponding enrichment plots are depicted to the right of each heatmap, with naïve lines in red (at the left of the plot) and primed lines in blue (at the right of the plot). All converted

naïve cell lines are shaded in grey, while their primed source counterparts are shaded in yellow. Red shades on the heatmaps depict upregulation, while blue shades depict downregulation. More significant upregulation/downregulation is indicated by darker tones of blue or red.

**Figure 13**

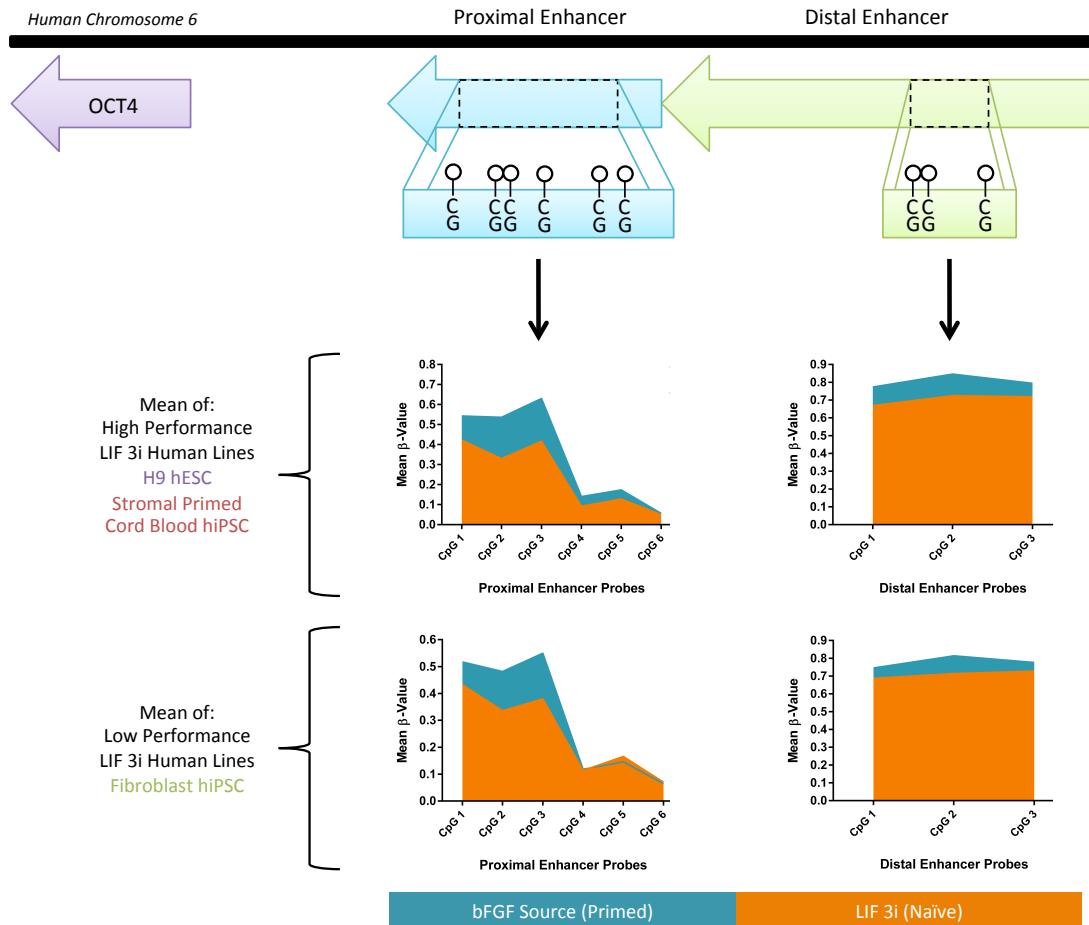


**Figure 13: DNA methylation profile across the human OCT4 proximal and distal enhancer elements for high performing and low performing lines**

Analysis of human Infinium 450k DNA methylation arrays from ground state LIF 3i and bFGF source pluripotent stem cells was conducted to investigate a possible proximal to distal enhancer regulatory switch upon LIF 3i naïve reversion. The 450k array has six probes examining six CpG sites within the OCT4 proximal enhancer, and three probes examining three CpG sites within the distal enhancer. Mean methylation beta values are indicated for high performing LIF 3i and source bFGF

lines (H9 hESC, stromal primed cord blood hiPSC) and low performing LIF 3i and bFGF source lines (fibroblast hiPSC).  $\beta = 1$  indicates a fully methylated CpG probe, while  $\beta = 0$  indicates a fully unmethylated CpG probe.



**Figure 14**

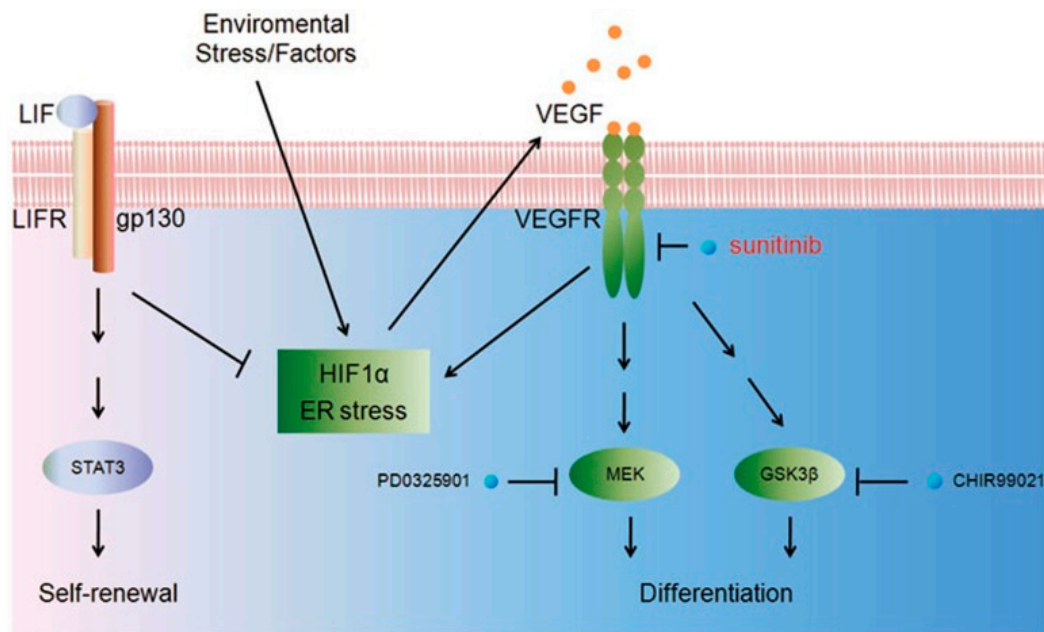


**Figure 14: Possible mechanisms surrounding VEGF receptor inhibition in rhesus mESC-like self-renewal**

LIF signaling through LIF receptor (LIFR) and gp130 activates STAT3 and classical mESC-like self-renewal. LIFR/gp130 activation may also have a secondary effect of inhibiting HIF1 $\alpha$ /endoplasmic reticulum (ER) stress. *In vitro* hypoxic culture and environmental stress (possibly including single cell dissociation) may act to increase VEGF ligand secretion and autocrine VEGF signaling via a HIF1 $\alpha$ /ER stress signaling axis. Blocking VEGF receptor (VEGFR) with sunitinib reinforces the combined effect of MEK inhibition and GSK3- $\beta$  inhibition to prevent rESC differentiation. Additionally, blocking VEGFRs with sunitinib may block the feed-forward loop between VEGFR activation and HIF1 $\alpha$ /ER stress, and act to minimize tendencies for rESCs to spontaneously differentiate in culture upon autocrine VEGF stimulation. Used unmodified from Chen et al. (2014)<sup>72</sup>.

## REFERENCES

1. Nichols, J. & Smith, A. Naive and primed pluripotent states. *Cell Stem Cell* **4**, 487–492 (2009).
2. Mascetti, V. L. & Pedersen, R. A. Naiveté of the human pluripotent stem cell. *Nat. Biotechnol.* **32**, 68–70 (2014).
3. Ying, Q.-L. *et al.* The ground state of embryonic stem cell self-renewal. *Nature* **453**, 519–523 (2008).
4. Hanna, J. H., Saha, K. & Jaenisch, R. Pluripotency and cellular reprogramming: facts, hypotheses, unresolved issues. *Cell* **143**, 508–525 (2010).
5. Brons, I. G. M. *et al.* Derivation of pluripotent epiblast stem cells from mammalian embryos. *Nature* **448**, 191–195 (2007).
6. Marks, H. *et al.* The transcriptional and epigenomic foundations of ground state pluripotency. *Cell* **149**, 590–604 (2012).
7. Tesar, P. J. *et al.* New cell lines from mouse epiblast share defining features with human embryonic stem cells. *Nature* **448**, 196–199 (2007).
8. Chia, N.-Y. *et al.* A genome-wide RNAi screen reveals determinants of human embryonic stem cell identity. *Nature* **468**, 316–320 (2010).
9. Hanna, J. *et al.* Human embryonic stem cells with biological and epigenetic characteristics similar to those of mouse ESCs. *Proc. Natl. Acad. Sci. U. S. A.* **107**, 9222–9227 (2010).
10. Hedges, S. B., Dudley, J. & Kumar, S. TimeTree: a public knowledge-base of divergence times among organisms. *Bioinforma. Oxf. Engl.* **22**, 2971–2972 (2006).

11. Nichols, J., Chambers, I., Taga, T. & Smith, A. Physiological rationale for responsiveness of mouse embryonic stem cells to gp130 cytokines. *Dev. Camb. Engl.* **128**, 2333–2339 (2001).
12. Kalkan, T. & Smith, A. Mapping the route from naive pluripotency to lineage specification. *Philos. Trans. R. Soc. Lond. B. Biol. Sci.* **369**, (2014).
13. Hanna, J. *et al.* Metastable pluripotent states in NOD-mouse-derived ESCs. *Cell Stem Cell* **4**, 513–524 (2009).
14. Guo, G. *et al.* Klf4 reverts developmentally programmed restriction of ground state pluripotency. *Dev. Camb. Engl.* **136**, 1063–1069 (2009).
15. Silva, J. *et al.* Nanog is the gateway to the pluripotent ground state. *Cell* **138**, 722–737 (2009).
16. Zaharevitz, D. W. *et al.* Discovery and initial characterization of the paullones, a novel class of small-molecule inhibitors of cyclin-dependent kinases. *Cancer Res.* **59**, 2566–2569 (1999).
17. Schultz, C. *et al.* Paullones, a series of cyclin-dependent kinase inhibitors: synthesis, evaluation of CDK1/cyclin B inhibition, and in vitro antitumor activity. *J. Med. Chem.* **42**, 2909–2919 (1999).
18. Leost, M. *et al.* Paullones are potent inhibitors of glycogen synthase kinase-3 $\beta$  and cyclin-dependent kinase 5/p25. *Eur. J. Biochem. FEBS* **267**, 5983–5994 (2000).
19. Lyssiotis, C. A. *et al.* Reprogramming of murine fibroblasts to induced pluripotent stem cells with chemical complementation of Klf4. *Proc. Natl. Acad. Sci. U. S. A.* **106**, 8912–8917 (2009).

20. Wang, W. *et al.* Rapid and efficient reprogramming of somatic cells to induced pluripotent stem cells by retinoic acid receptor gamma and liver receptor homolog 1. *Proc. Natl. Acad. Sci. U. S. A.* **108**, 18283–18288 (2011).
21. Gafni, O. *et al.* Derivation of novel human ground state naive pluripotent stem cells. *Nature* **504**, 282–286 (2013).
22. Chan, Y.-S. *et al.* Induction of a human pluripotent state with distinct regulatory circuitry that resembles preimplantation epiblast. *Cell Stem Cell* **13**, 663–675 (2013).
23. Valamehr, B. *et al.* Platform for induction and maintenance of transgene-free hiPSCs resembling ground state pluripotent stem cells. *Stem Cell Rep.* **2**, 366–381 (2014).
24. Ware, C. B. *et al.* Derivation of naive human embryonic stem cells. *Proc. Natl. Acad. Sci. U. S. A.* **111**, 4484–4489 (2014).
25. Theunissen, T. W. *et al.* Systematic identification of culture conditions for induction and maintenance of naive human pluripotency. *Cell Stem Cell* **15**, 471–487 (2014).
26. Takashima, Y. *et al.* Resetting transcription factor control circuitry toward ground-state pluripotency in human. *Cell* **158**, 1254–1269 (2014).
27. Fang, R. *et al.* Generation of naive induced pluripotent stem cells from rhesus monkey fibroblasts. *Cell Stem Cell* **15**, 488–496 (2014).
28. Van Oosten, A. L., Costa, Y., Smith, A. & Silva, J. C. R. JAK/STAT3 signalling is sufficient and dominant over antagonistic cues for the establishment of naive pluripotency. *Nat. Commun.* **3**, 817 (2012).

29. Dutta, D. *et al.* Self-renewal versus lineage commitment of embryonic stem cells: protein kinase C signaling shifts the balance. *Stem Cells Dayt. Ohio* **29**, 618–628 (2011).
30. Hanna – Protocols. at <[http://hannalabweb.weizmann.ac.il/?page\\_id=129](http://hannalabweb.weizmann.ac.il/?page_id=129)>
31. Ying, Q.-L., Stavridis, M., Griffiths, D., Li, M. & Smith, A. Conversion of embryonic stem cells into neuroectodermal precursors in adherent monoculture. *Nat. Biotechnol.* **21**, 183–186 (2003).
32. Ying, Q. L., Nichols, J., Chambers, I. & Smith, A. BMP induction of Id proteins suppresses differentiation and sustains embryonic stem cell self-renewal in collaboration with STAT3. *Cell* **115**, 281–292 (2003).
33. Wiles, M. V. & Johansson, B. M. Embryonic stem cell development in a chemically defined medium. *Exp. Cell Res.* **247**, 241–248 (1999).
34. Malaguti, M. *et al.* Bone morphogenic protein signalling suppresses differentiation of pluripotent cells by maintaining expression of E-Cadherin. *eLife* **2**, e01197 (2013).
35. Zhang, K. *et al.* Distinct functions of BMP4 during different stages of mouse ES cell neural commitment. *Dev. Camb. Engl.* **137**, 2095–2105 (2010).
36. Davies, O. R. *et al.* Tcf15 primes pluripotent cells for differentiation. *Cell Rep.* **3**, 472–484 (2013).
37. Huang, S.-M. A. *et al.* Tankyrase inhibition stabilizes axin and antagonizes Wnt signalling. *Nature* **461**, 614–620 (2009).
38. Kim, H. *et al.* Modulation of  $\beta$ -catenin function maintains mouse epiblast stem cell and human embryonic stem cell self-renewal. *Nat. Commun.* **4**, 2403 (2013).

39. Chen, B. *et al.* Small molecule-mediated disruption of Wnt-dependent signaling in tissue regeneration and cancer. *Nat. Chem. Biol.* **5**, 100–107 (2009).
40. Faunes, F. *et al.* A membrane-associated  $\beta$ -catenin/Oct4 complex correlates with ground-state pluripotency in mouse embryonic stem cells. *Dev. Camb. Engl.* **140**, 1171–1183 (2013).
41. Marucci, L. *et al.*  $\beta$ -catenin fluctuates in mouse ESCs and is essential for Nanog-mediated reprogramming of somatic cells to pluripotency. *Cell Rep.* **8**, 1686–1696 (2014).
42. Zwaka, T. P. & Thomson, J. A. Homologous recombination in human embryonic stem cells. *Nat. Biotechnol.* **21**, 319–321 (2003).
43. Irion, S. *et al.* Identification and targeting of the ROSA26 locus in human embryonic stem cells. *Nat. Biotechnol.* **25**, 1477–1482 (2007).
44. Davis, R. P. *et al.* Targeting a GFP reporter gene to the MIXL1 locus of human embryonic stem cells identifies human primitive streak-like cells and enables isolation of primitive hematopoietic precursors. *Blood* **111**, 1876–1884 (2008).
45. Ruby, K. M. & Zheng, B. Gene targeting in a HUES line of human embryonic stem cells via electroporation. *Stem Cells Dayt. Ohio* **27**, 1496–1506 (2009).
46. Xue, H. *et al.* A targeted neuroglial reporter line generated by homologous recombination in human embryonic stem cells. *Stem Cells Dayt. Ohio* **27**, 1836–1846 (2009).
47. Ishii, A., Kurosawa, A., Saito, S. & Adachi, N. Analysis of the role of homology arms in gene-targeting vectors in human cells. *PloS One* **9**, e108236 (2014).

48. Alba, R., Bosch, A. & Chillon, M. Gutless adenovirus: last-generation adenovirus for gene therapy. *Gene Ther.* **12 Suppl 1**, S18–27 (2005).
49. Li, M., Suzuki, K., Kim, N. Y., Liu, G.-H. & Izpisua Belmonte, J. C. A cut above the rest: targeted genome editing technologies in human pluripotent stem cells. *J. Biol. Chem.* **289**, 4594–4599 (2014).
50. Smith, S., Gariat, I., Schmitt, A. & de Lange, T. Tankyrase, a poly(ADP-ribose) polymerase at human telomeres. *Science* **282**, 1484–1487 (1998).
51. Cook, B. D., Dynek, J. N., Chang, W., Shostak, G. & Smith, S. Role for the related poly(ADP-Ribose) polymerases tankyrase 1 and 2 at human telomeres. *Mol. Cell. Biol.* **22**, 332–342 (2002).
52. Bristow, R. G. & Hill, R. P. Hypoxia and metabolism. Hypoxia, DNA repair and genetic instability. *Nat. Rev. Cancer* **8**, 180–192 (2008).
53. Weterings, E. & Chen, D. J. The endless tale of non-homologous end-joining. *Cell Res.* **18**, 114–124 (2008).
54. Dregalla, R. C. *et al.* Regulatory roles of tankyrase 1 at telomeres and in DNA repair: suppression of T-SCE and stabilization of DNA-PKcs. *Aging* **2**, 691–708 (2010).
55. Paulk, N. K., Loza, L. M., Finegold, M. J. & Grompe, M. AAV-mediated gene targeting is significantly enhanced by transient inhibition of nonhomologous end joining or the proteasome in vivo. *Hum. Gene Ther.* **23**, 658–665 (2012).
56. Durant, S. & Karran, P. Vanillins--a novel family of DNA-PK inhibitors. *Nucleic Acids Res.* **31**, 5501–5512 (2003).
57. Ohta, T. Modification of genotoxicity by naturally occurring flavorings and their derivatives. *Crit. Rev. Toxicol.* **23**, 127–146 (1993).

58. Watanabe, K., Ohta, T., Watanabe, M., Kato, T. & Shirasu, Y. Inhibition of induction of adaptive response by o-vanillin in *Escherichia coli* B. *Mutat. Res.* **243**, 273–280 (1990).
59. Keshava, C., Keshava, N., Ong, T. M. & Nath, J. Protective effect of vanillin on radiation-induced micronuclei and chromosomal aberrations in V79 cells. *Mutat. Res.* **397**, 149–159 (1998).
60. Gustafson, D. L. *et al.* Vanillin (3-methoxy-4-hydroxybenzaldehyde) inhibits mutation induced by hydrogen peroxide, N-methyl-N-nitrosoguanidine and mitomycin C but not (137)Cs gamma-radiation at the CD59 locus in human-hamster hybrid A(L) cells. *Mutagenesis* **15**, 207–213 (2000).
61. Maurya, D. K., Adhikari, S., Nair, C. K. K. & Devasagayam, T. P. A. DNA protective properties of vanillin against gamma-radiation under different conditions: possible mechanisms. *Mutat. Res.* **634**, 69–80 (2007).
62. Rashid, T., Kobayashi, T. & Nakauchi, H. Revisiting the flight of Icarus: making human organs from PSCs with large animal chimeras. *Cell Stem Cell* **15**, 406–409 (2014).
63. Tachibana, M. *et al.* Generation of chimeric rhesus monkeys. *Cell* **148**, 285–295 (2012).
64. Kobayashi, T. *et al.* Generation of rat pancreas in mouse by interspecific blastocyst injection of pluripotent stem cells. *Cell* **142**, 787–799 (2010).
65. Usui, J. *et al.* Generation of kidney from pluripotent stem cells via blastocyst complementation. *Am. J. Pathol.* **180**, 2417–2426 (2012).
66. Isotani, A., Hatayama, H., Kaseda, K., Ikawa, M. & Okabe, M. Formation of a thymus from rat ES cells in xenogeneic nude mouse↔rat ES chimeras. *Genes Cells Devoted Mol. Cell. Mech.* **16**, 397–405 (2011).



67. Matsunari, H. *et al.* Blastocyst complementation generates exogenic pancreas in vivo in apancreatic cloned pigs. *Proc. Natl. Acad. Sci. U. S. A.* **110**, 4557–4562 (2013).
68. Kobayashi, T., Kato-Itoh, M. & Nakauchi, H. Targeted organ generation using Mixl1-inducible mouse pluripotent stem cells in blastocyst complementation. *Stem Cells Dev.* **24**, 182–189 (2015).
69. Mitalipov, S. *et al.* Isolation and characterization of novel rhesus monkey embryonic stem cell lines. *Stem Cells Dayt. Ohio* **24**, 2177–2186 (2006).
70. Byrne, J. A. *et al.* Producing primate embryonic stem cells by somatic cell nuclear transfer. *Nature* **450**, 497–502 (2007).
71. Dighe, V. *et al.* Heterozygous embryonic stem cell lines derived from nonhuman primate parthenotes. *Stem Cells Dayt. Ohio* **26**, 756–766 (2008).
72. Chen, G. *et al.* Blocking autocrine VEGF signaling by sunitinib, an anti-cancer drug, promotes embryonic stem cell self-renewal and somatic cell reprogramming. *Cell Res.* **24**, 1121–1136 (2014).
73. Forristal, C. E., Wright, K. L., Hanley, N. A., Oreffo, R. O. C. & Houghton, F. D. Hypoxia inducible factors regulate pluripotency and proliferation in human embryonic stem cells cultured at reduced oxygen tensions. *Reprod. Camb. Engl.* **139**, 85–97 (2010).
74. Wang, Q. *et al.* Lithium, an anti-psychotic drug, greatly enhances the generation of induced pluripotent stem cells. *Cell Res.* **21**, 1424–1435 (2011).
75. Subramanian, A. *et al.* Gene set enrichment analysis: a knowledge-based approach for interpreting genome-wide expression profiles. *Proc. Natl. Acad. Sci. U. S. A.* **102**, 15545–15550 (2005).

76. Allegrucci, C. *et al.* Human embryonic stem cells as a model for nutritional programming: an evaluation. *Reprod. Toxicol. Elmsford N* **20**, 353–367 (2005).
77. Skottman, H. *et al.* Gene expression signatures of seven individual human embryonic stem cell lines. *Stem Cells Dayt. Ohio* **23**, 1343–1356 (2005).
78. International Stem Cell Initiative *et al.* Characterization of human embryonic stem cell lines by the International Stem Cell Initiative. *Nat. Biotechnol.* **25**, 803–816 (2007).
79. Allegrucci, C. & Young, L. E. Differences between human embryonic stem cell lines. *Hum. Reprod. Update* **13**, 103–120 (2007).
80. Osafune, K. *et al.* Marked differences in differentiation propensity among human embryonic stem cell lines. *Nat. Biotechnol.* **26**, 313–315 (2008).
81. Choi, K.-D. *et al.* Hematopoietic and endothelial differentiation of human induced pluripotent stem cells. *Stem Cells Dayt. Ohio* **27**, 559–567 (2009).
82. Hu, B.-Y. *et al.* Neural differentiation of human induced pluripotent stem cells follows developmental principles but with variable potency. *Proc. Natl. Acad. Sci. U. S. A.* **107**, 4335–4340 (2010).
83. Feng, Q. *et al.* Hemangioblastic derivatives from human induced pluripotent stem cells exhibit limited expansion and early senescence. *Stem Cells Dayt. Ohio* **28**, 704–712 (2010).
84. Boulting, G. L. *et al.* A functionally characterized test set of human induced pluripotent stem cells. *Nat. Biotechnol.* **29**, 279–286 (2011).
85. Waddington, C. H. *The Strategy of the Genes. A Discussion of Some Aspects of Theoretical Biology.* With an appendix by H. Kacser. ix +262 pp. (1957).
86. Goldberg, A. D., Allis, C. D. & Bernstein, E. Epigenetics: a landscape takes shape. *Cell* **128**, 635–638 (2007).

87. Zhang, J. *et al.* BMP induces cochlin expression to facilitate self-renewal and suppress neural differentiation of mouse embryonic stem cells. *J. Biol. Chem.* **288**, 8053–8060 (2013).
88. Onishi, K., Tonge, P. D., Nagy, A. & Zandstra, P. W. Local BMP-SMAD1 signaling increases LIF receptor-dependent STAT3 responsiveness and primed-to-naïve mouse pluripotent stem cell conversion frequency. *Stem Cell Rep.* **3**, 156–168 (2014).
89. Tonge, P. D. *et al.* Divergent reprogramming routes lead to alternative stem-cell states. *Nature* **516**, 192–197 (2014).
90. Shimizu, T. *et al.* Dual inhibition of Src and GSK3 maintains mouse embryonic stem cells, whose differentiation is mechanically regulated by Src signaling. *Stem Cells Dayt. Ohio* **30**, 1394–1404 (2012).
91. Wolf, D. P. *et al.* Use of assisted reproductive technologies in the propagation of rhesus macaque offspring. *Biol. Reprod.* **71**, 486–493 (2004).
92. Ezashi, T., Das, P. & Roberts, R. M. Low O<sub>2</sub> tensions and the prevention of differentiation of hES cells. *Proc. Natl. Acad. Sci. U. S. A.* **102**, 4783–4788 (2005).
93. Han, Y., Kuang, S.-Z., Gomer, A. & Ramirez-Bergeron, D. L. Hypoxia influences the vascular expansion and differentiation of embryonic stem cell cultures through the temporal expression of vascular endothelial growth factor receptors in an ARNT-dependent manner. *Stem Cells Dayt. Ohio* **28**, 799–809 (2010).
94. Lee, S.-W. *et al.* Hypoxic priming of mESCs accelerates vascular-lineage differentiation through HIF1-mediated inverse regulation of Oct4 and VEGF. *EMBO Mol. Med.* **4**, 924–938 (2012).

95. Mazumdar, J. *et al.* O<sub>2</sub> regulates stem cells through Wnt/ $\beta$ -catenin signalling. *Nat. Cell Biol.* **12**, 1007–1013 (2010).
96. Kubota, Y., Hirashima, M., Kishi, K., Stewart, C. L. & Suda, T. Leukemia inhibitory factor regulates microvessel density by modulating oxygen-dependent VEGF expression in mice. *J. Clin. Invest.* **118**, 2393–2403 (2008).
97. Conley, S. J. *et al.* Antiangiogenic agents increase breast cancer stem cells via the generation of tumor hypoxia. *Proc. Natl. Acad. Sci. U. S. A.* **109**, 2784–2789 (2012).
98. Yusa, K. *et al.* Targeted gene correction of  $\alpha$ 1-antitrypsin deficiency in induced pluripotent stem cells. *Nature* **478**, 391–394 (2011).
99. Zou, J., Mali, P., Huang, X., Dowey, S. N. & Cheng, L. Site-specific gene correction of a point mutation in human iPS cells derived from an adult patient with sickle cell disease. *Blood* **118**, 4599–4608 (2011).
100. Yusa, K. Seamless genome editing in human pluripotent stem cells using custom endonuclease-based gene targeting and the piggyBac transposon. *Nat. Protoc.* **8**, 2061–2078 (2013).
101. Sun, N. & Zhao, H. Seamless correction of the sickle cell disease mutation of the HBB gene in human induced pluripotent stem cells using TALENs. *Biotechnol. Bioeng.* **111**, 1048–1053 (2014).
102. Xie, F. *et al.* Seamless gene correction of  $\beta$ -thalassemia mutations in patient-specific iPSCs using CRISPR/Cas9 and piggyBac. *Genome Res.* **24**, 1526–1533 (2014).
103. Dunn, S.-J., Martello, G., Yordanov, B., Emmott, S. & Smith, A. G. Defining an essential transcription factor program for naïve pluripotency. *Science* **344**, 1156–1160 (2014).

104. Huang, K., Maruyama, T. & Fan, G. The naive state of human pluripotent stem cells: a synthesis of stem cell and preimplantation embryo transcriptome analyses. *Cell Stem Cell* **15**, 410–415 (2014).
105. Takahashi, K. & Yamanaka, S. Induction of pluripotent stem cells from mouse embryonic and adult fibroblast cultures by defined factors. *Cell* **126**, 663–676 (2006).
106. Barth, T. K. & Imhof, A. Fast signals and slow marks: the dynamics of histone modifications. *Trends Biochem. Sci.* **35**, 618–626 (2010).
107. Martello, G. & Smith, A. The Nature of Embryonic Stem Cells. *Annu. Rev. Cell Dev. Biol.* **30**, 647–675 (2014).
108. Robinton, D. A. & Daley, G. Q. The promise of induced pluripotent stem cells in research and therapy. *Nature* **481**, 295–305 (2012).
109. Park, T. S. *et al.* Growth factor-activated stem cell circuits and stromal signals cooperatively accelerate non-integrated iPSC reprogramming of human myeloid progenitors. *PloS One* **7**, e42838 (2012).
110. The 2007 Nobel Prize in Physiology or Medicine - Advanced Information. at <[http://www.nobelprize.org/nobel\\_prizes/medicine/laureates/2007/advanced.html](http://www.nobelprize.org/nobel_prizes/medicine/laureates/2007/advanced.html)>
111. Kim, H. & Kim, J.-S. A guide to genome engineering with programmable nucleases. *Nat. Rev. Genet.* **15**, 321–334 (2014).

## CURRICULUM VITAE

### **Sarshan Rubintheran Pather**

Date of Birth: 14<sup>th</sup> November 1994 (Age 20)

Birthplace: Durban, South Africa

Nationality: South African

Email Address: [spather1@jhu.edu](mailto:spather1@jhu.edu)

---

### **Education**

2014 - 2015: M.S. Molecular and Cellular Biology (GPA: 4.00)  
The Zambidis Laboratory  
Johns Hopkins University

2012 - 2013: Hopkins-St. Anne's Pre-Medical Honors Program  
Molecular and Cellular Biochemistry  
University of Oxford

2011 - 2014: B.S. Molecular and Cellular Biology (with Honors; GPA: 3.97)  
Johns Hopkins University

2009 - 2011: Singapore American School (GPA: 4.11)  
Singapore

### **Work Experience**

2013 - 2015: Research Assistant in Stem Cell Biology  
The Zambidis Laboratory  
Johns Hopkins University School of Medicine

2014 - 2015: Teaching Assistant, General Biology (Lecture and Laboratory)  
Johns Hopkins University

2013: Oncology Shadowing (with Dr. Elias T. Zambidis, MD/PhD)  
Johns Hopkins University School of Medicine

2012: Accident and Emergency Trauma Unit Medical Orderly  
Chatsmed Garden Hospital, Durban, South Africa

2011: General Surgery Shadowing  
Chatsmed Garden Hospital, Durban, South Africa

**Volunteer Service and Leadership**  
*(During B.S. and M.S. Degrees)*

President of JHU GED Tutoring  
President of JHU Golden Key International Honor Society  
JHU American Red Cross

**Society Memberships**

Member of:

Beta Beta Beta (Tri-Beta) National Biological Honor Society  
*Presented B.S. Honors Thesis at the Tri-Beta Poster Session (2014)*  
Phi Beta Kappa  
Golden Key International Honor Society  
Oxford University Scientific Society

**Music and Athletic Achievement**

Grade 5 Piano Certificate  
*Associated Board of the Royal Schools of Music*  
Grade 5 Alto Saxophone Certificate  
*Associated Board of the Royal Schools of Music*

JHU Jazz Band  
JHU Golf Club  
Oxford University and St. Anne's College 1<sup>st</sup>/2<sup>nd</sup> XI Cricket Team

---